

CHAPTER 1

INTRODUCTION

1.1 PROBLEM STATEMENT

The history of the MAV starts in the 19 century; researches had been carried out in all the big countries like the Unites States, Japan, China. So what are we trying to do in the final year project is to try to understand more and more about the aerodynamics of the MAV and how to make it work so it can help other countries all over the world.[1]

The most common problem that faces an unmanned aerial vehicle is having a low Reynolds number. MAV has a low Reynolds number because of its small size. Results indicate an increase in maximum lift coefficient with decreasing Reynolds number, but the lift to drag ratio continues to decrease making the power required for flight a more restrictive consideration than lift. [2]

Flight at these Reynolds numbers is much less efficient than at higher Reynolds numbers and available power is a limiting technological factor at small scales. It is important to operate the airfoil at its maximum L/D operating point. [2]

Flow at low Reynolds numbers is dominated by viscosity, and as the Reynolds number is reduced, the effects of increasing boundary layer thickness become more pronounced. It will also bring effect to a higher drag. [2]

1.2 OBJECTIVES

The main objective of this research is fabricating a MAV and experiment it in the wind tunnel.

- Understanding the fundamentals of flight
- studying the aerodynamics characteristics
- understanding the wind tunnel testing
- improving the design to enhance the aerodynamics characteristics

1.3 BACKGROUND OF STUDY

1.3.1 MICRO AERIAL VEHICLE

Micro Aerial Vehicle, also known as a drone, it is an aircraft without a human operator on board. The largest modern micro aerial vehicles (MAVs) have a wingspan of more than 30 m; the smallest MAVs can be carried in a backpack. MAVs originated during World War I (1914-1918), but modern MAVs were first developed in the 1970s. [3]

In the near future, MAVs are expected to be used for civilian missions as well. The United States Coast Guard planned to use MAVs for search, rescue, and patrol operations. MAVs could also be used for aerial surveys and to inspect pipelines and power lines—jobs done today by piloted airplanes. [3]

MAVs are flown and navigated by onboard computers and operated by humans on the ground. Software code containing the entire mission plan is downloaded to the MAV's computers before it is launched. The operator on the ground does not “fly” the UAV, but can change the mission plan by sending new software instructions to the computers via

radio, so that the MAV will change course, circle a target, or return to base. The MAV will continue to fly even if it loses radio contact with the operator, who may be hundreds or even thousands of kilometers away. [3]

Different MAVs can be different in terms of size, shapes and configurations, depending on the design. A few types of MAVs are shown.



FIGURE 1.1: example of UAV-PREDATOR 1 [4]



FIGURE 1.2: example of a UAV- RQ-4A GLOBAL HAWK [5]



FIGURE 1.3: Example of medium size UAV-hunter 1 [6]



FIGURE 1.4: Example of medium size UAV-MAIDEN [7]

Almost all MAVs are military aircraft. Most of them are used for reconnaissance (exploration to gather information), although a few MAVs are armed with missiles. MAVs are employed when a piloted reconnaissance aircraft would run a high risk of being attacked or for very long missions that would exceed a pilot's physical endurance. Often, a MAV is smaller and cheaper than a piloted aircraft designed to do the same job.

1.3.2 FORCES ACTING ON A FLIGHT

There are, basically, four forces of flight: lift, drag, thrust and weight. The figure below shows how these four forces are related for straight and level flight. Lift force point upward, opposite to the weight. Thrust pushes the plane forward, as drag slows it down. The lift force must be greater than the weight and the thrust more powerful than the drag for the plane to fly.

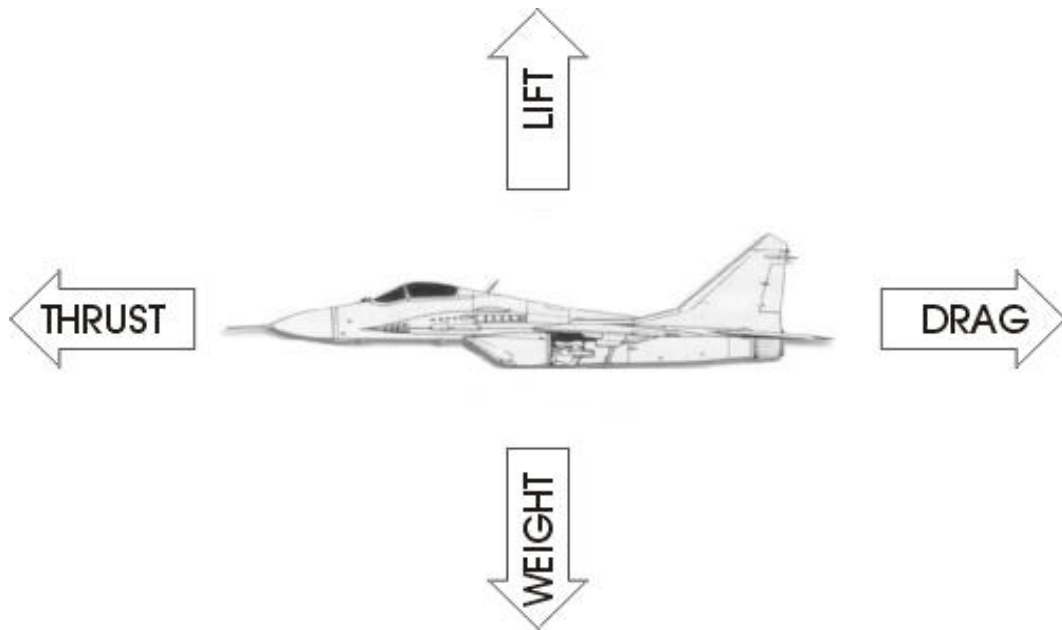


FIGURE 1.5: forces acting on a flight [8]

Lift and Drag are considered aerodynamic forces because they exist due to the movement of the aircraft through the air.

Weight

Weight is present because of gravity. Gravity is a natural force that pulls the plane down towards the earth. Therefore, the direction of weight is down. [9]

Lift force:

The force that pushes an object up against the weight is lift. On an airplane, the lift is created by the movement of the air around the wings. Air moves over the top and bottom of the wing at different speeds to create lift. There are two ways to do this. The wing itself can have a curved upper surface and flatter lower surface. This forces the air flowing over the top of the wing to move faster. This creates lift. Another way is to use a flat wing and fly at an angle to the wind. The slanted wing causes the air to move more quickly over the top of it, creating lift. [9]

Modern aircraft have a curved upper surface on the wing. The figure below shows two streamlines; one is going over the wing and the other under the wing. The faster air leads to low pressure on top of the wing and the slower stream under the wing creates a higher pressure. The two together produce lift. [9]

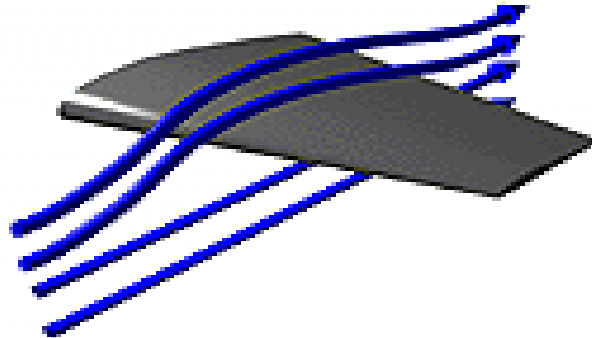


FIGURE 1.6: Curved upper surface on the wing [10]

According to Newton's Third Law, for every action there is an equal, but opposite reaction. Therefore, if the airfoil deflects the air down, the resulting opposite reaction is an upward

push. Deflection is an important source of lift. Planes with flat wings, rather than cambered, or curved wings must tilt their wings to get deflection. [9]

Thrust

Thrust is created by airplane engines .The engines can turn a propeller at high speed or can be a jet engine that pushes hot gases out the back. If the thrust is powerful enough it will overcome weight and drag and the plane will fly. [9]

Drag

Drag is the force which delays or slows the forward movement of an airplane through the air when the airflow direction is opposite to the direction of motion of the airplane. It is the friction of the air as it meets and passes over and about an airplane and its components. The more surface area exposed to rushing air, the greater the drag. An airplane's streamlined shape helps it pass through the air more easily. [9]

There are four types of drag:

1. Friction drag - As an airplane goes through the air, the air must go around the plane. The air is "rubbing" against the metal skin of the aircraft. This tends to slow the aircraft.
2. Form drag - The shape of the airplane can make more or less drag. If the plane is "streamlined" the air will pass around it with less drag. Think of a truck or a bus. The flat front is not streamlined. This creates more drag, and more fuel is used. Put your hand out the window of a car, palm forward, this is an example of the form of a bus or truck. Feel the drag!
3. Induced drag - When lift is created around a wing, drag is also created.
4. Wave drag - When an airplane is flying near or faster than the speed of sound the air flow around the aircraft changes and becomes an additional drag. [9]

1.3.3 LIFT AND DRAG COEFFICIENT

In aerodynamics, the most important non-dimensional quantities are Reynolds number and Mach number. Reynolds number is the ratio inertial and viscous forces and Mach number is the ratio of airspeed to the speed of sound.

In an aircraft configuration, the force coefficient (lift and drag coefficient) is shown to be dependent on Mach number (M), Reynolds number (Re), angle of attack (α) and the geometry shape of the aircraft (t). The relationship between the force coefficient and those parameters mentioned is shown in the following equation. [11]

$$C_L = C_L(\alpha, Re, M, t)$$

$$C_D = C_D(\alpha, Re, M, t)$$

The lift coefficient can be represented by the following equations: [12]

$$C_L = \frac{F_l}{\frac{1}{2}\rho v^2 A}$$

Where C_L lift coefficient, w is weight of the vehicle, ρ is the air density, V is the relative velocity and A is the reference area.

The drag coefficient can be represented by the following equations: [12]

$$C_d = \frac{F_d}{\frac{1}{2}\rho v^2 A}$$

Where F_D is the drag force, which is by definition the force component in the direction of the flow velocity, ρ is the mass density of the fluid, V is the speed of the object relative to the fluid, and A is the reference area.

The drag in any airplane maybe derived from the tangential actions of fluid reactions on the external skin. The pressure component of an asymptotic velocity resulting from the actions produced over the body is called pressure drag.

Induced drag is a drag force that occurs whenever a moving object redirects the airflow coming at it. This drag force occurs in airplanes due to wings or a lifting body redirecting air to cause lift and also in cars with airfoil wings that redirect air to cause a down force. With other parameters remaining the same, as the angle of attack increases, induced drag increases. [12]

The sum of the friction drag, stream drag and wave drag is called profile drag. [12]

$$C_D = C_{D_p} + C_{D_i}$$

It is very difficult to get an accurate calculation to the drag profile, due to the complex forms of air craft, due to the multiple components they have and the different flow conditions they subjected to, so the best option is to test in the wind tunnel which will give more accurate results.

The lift is directly proportional with angle of attack, which means when the angle of attack increases the lift coefficient increases, but when the angle of attack exceeds a specific angle the lift coefficient starts to decrease, this condition is called Stall. [13]

A stall is a condition in aerodynamics and aviation where the angle of attack increases beyond a certain point such that the lift begins to decrease. The angle at which this occurs is called the critical angle of attack. This critical angle is dependent upon the profile of the wing, its platform, its aspect ratio, and other factors, but is typically in the range of 8 to 20 degrees relative to the incoming wind for most subsonic airfoils. The critical angle of attack is the angle of attack on the lift coefficient versus angle-of-attack curve at which the maximum lift coefficient occurs. [13]

It is a reduction in the lift coefficient generated by an airfoil as angle of attack increases. This occurs when the critical angle of attack of the airfoil is exceeded. The critical angle of attack is typically about 15 degrees, but it may vary significantly depending on the airfoil and Reynolds number. [13]

1.3.4 WIND TUNNEL TESTING

The Wright brothers were the first to plan and carry out a large and systematic series of airfoil wind tunnel test. Their tunnel was built in 1901; it was 6 ft long and had a 16-in square cross section. The flow is produced by a two bladed fan powered by a gasoline engine. [14]

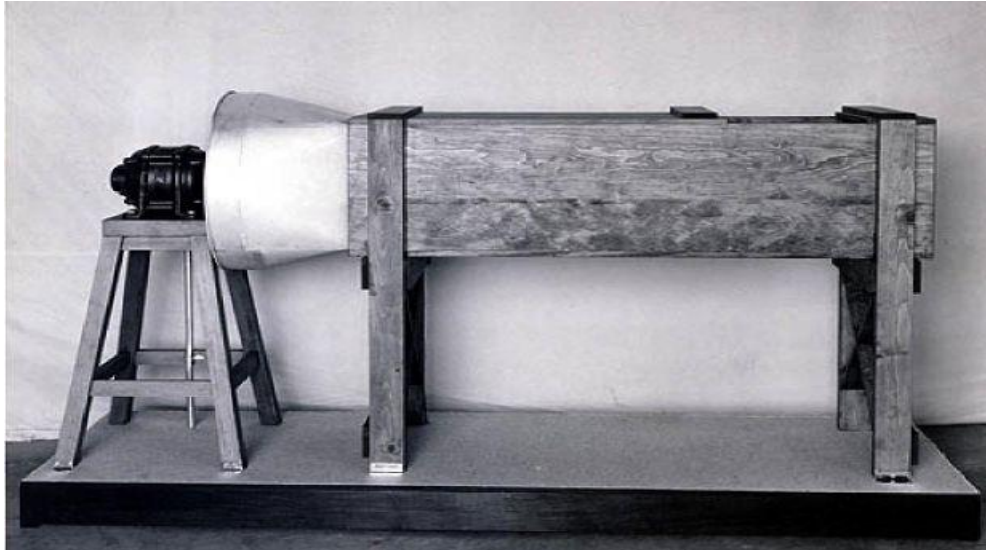


FIGURE 1.7: The Wright brothers' wind tunnel

Wind tunnel works as follow: Air is blown or sucked through a duct equipped with a viewing port and instrumentation where models or geometrical shapes are mounted for study. Typically the air is moved through the tunnel using a series of fans. For very large wind tunnels several meters in diameter, a single large fan is not practical, and so instead an array of multiple fans are used in parallel to provide sufficient airflow. Due to the sheer volume and speed of air movement required, the fans may be powered by stationary turbofan engines rather than electric motors.

The airflow created by the fans that is entering the tunnel is itself highly turbulent due to the fan blade motion (when the fan is blowing air into the test section - when it is sucking air out of the test section downstream, the fan-blade turbulence is not a factor), and so is not directly useful for accurate measurements. The air moving through the tunnel needs to be relatively turbulence-free and laminar. To correct this problem, closely-spaced vertical and horizontal air vanes are used to smooth out the turbulent airflow before reaching the subject of the testing.

Due to the effects of viscosity, the cross-section of a wind tunnel is typically circular rather than square, because there will be greater flow constriction in the corners of a square tunnel that can make the flow turbulent. A circular tunnel provides a smoother flow. [14]

The inside facing of the tunnel is typically as smooth as possible, to reduce surface drag and turbulence that could impact the accuracy of the testing. Even smooth walls induce some drag into the airflow, and so the object being tested is usually kept near the center of the tunnel, with an empty buffer zone between the object and the tunnel walls. There are correction factors to relate wind tunnel test results to open-air results. [14]

From wind tunnel testing, a few data can be retrieved. For example drag polar, pressure and flow visualization. Drag polar represents wing efficiency from induced drag and lift. Pressure can be used to determine flow separation on a surface, calculate local forces and to supply validation for numerical testing.

CHAPTER 2

LITERATURE REVIEW

Researches` have been made on UAVs, its control systems and aerodynamics characteristics by using computational and experimental methods.

In a journal named “aerodynamic characteristics of two rotary wings UAV”, the primary goal of the investigation was to provide a set of interactional aerodynamic data for an emerging class of rotorcraft, an experimental investigation of two rotary-wing UAV designs was conducted. A wing was designed along with these configurations in order to explore the effects of wing lift on configuration aerodynamics and to provide mount points for rockets. As with the fuselage shapes, the wing was designed to be a simple geometric shape in order to insure ease of modeling. The wing layout was developed by following the description; the resulting wing layout is a simple linearly tapered shape, employing a NACA 23012 airfoil, and no twist. The wing span is 48.4 in. The root chord is 6.55 in and the tip chord is 4.7 in yielding a taper ratio of 0.717. The wing aspect ratio is 4.3 and overall wing area is $271.8in^2$. The results of lift and drag coefficients versus angle of attack are shown in the following tables. [15]

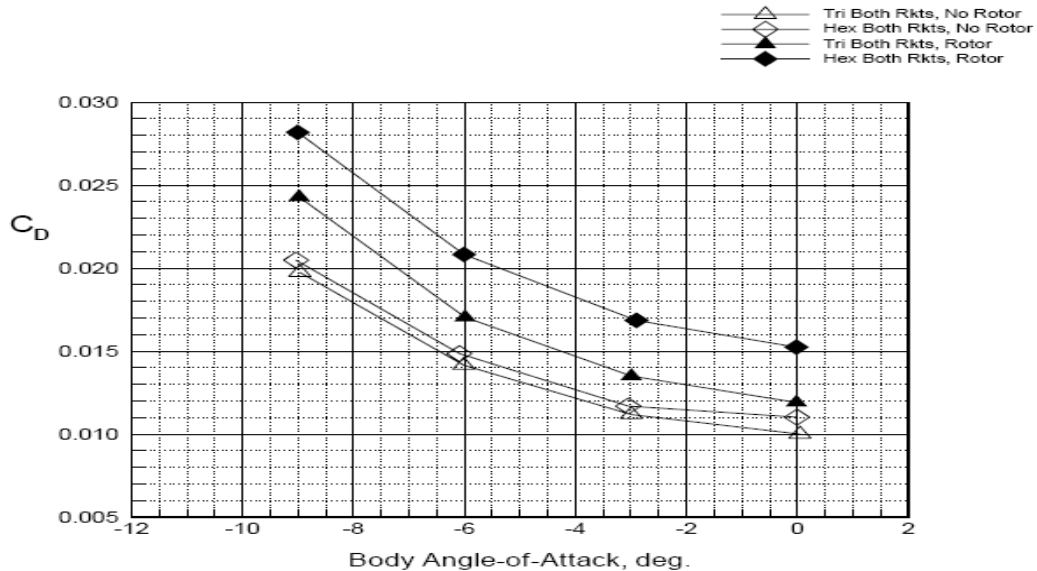


FIGURE 2.1: Variation of drag coefficient with angle-of-attack for basic configurations plus the wing, a rocket with and without the rotor, $\beta = 00$, $V = 100$ knots. [15]

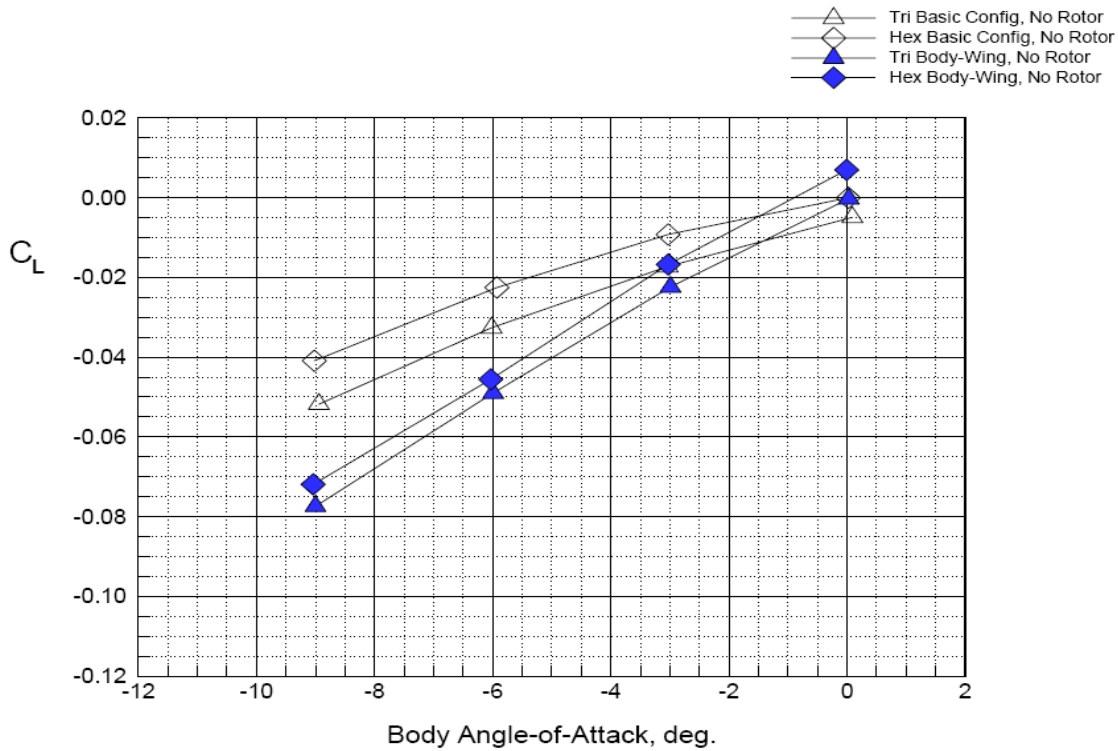


FIGURE 2.2: Variation of lift coefficient with angle-of-attack for basic configurations plus the wing, and rockets with and without the rotor, $\beta = 00$, $V = 100$ knots [15]

In this paper published by “University of Notre Dame” there are some of the results of an experimental investigation on low Reynolds number aerodynamics of small low-aspect-ratio wings. For this investigation, several thin, and cambered rectangular aluminum models with a thickness-to chord ratio of 1.93% were built. Thin models were selected, which glide at low Reynolds numbers, have very thin wings. The models had either a 5-to-1 elliptical leading edge and a 3-deg tapered trailing edge or a 5-to-1 elliptical leading edge and trailing edge. The cambered models had a circular arc shape with 4% camber. The semi span aspect ratios tested varied between 0.50 and 3.00. In this paper it shows the results of lift, drag and pitching moment coefficients and with the variation of angle of attack and semi span ratios. [17]

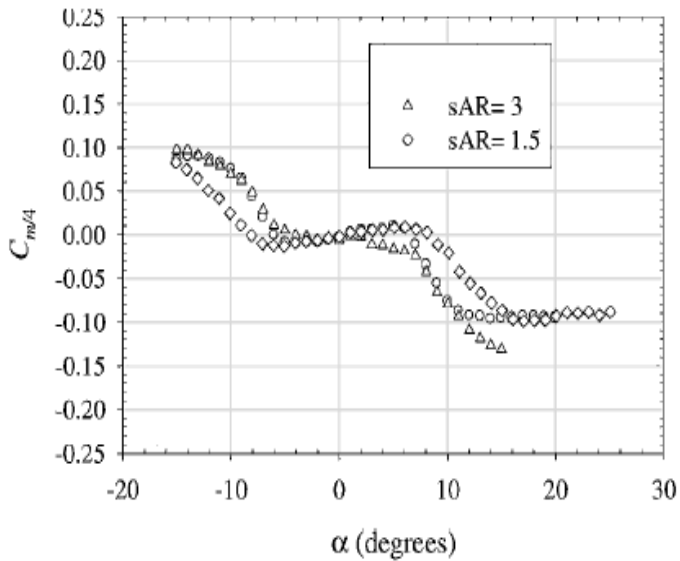


FIGURE 2.3: pitching moment coefficient Vs angle of attack [17]

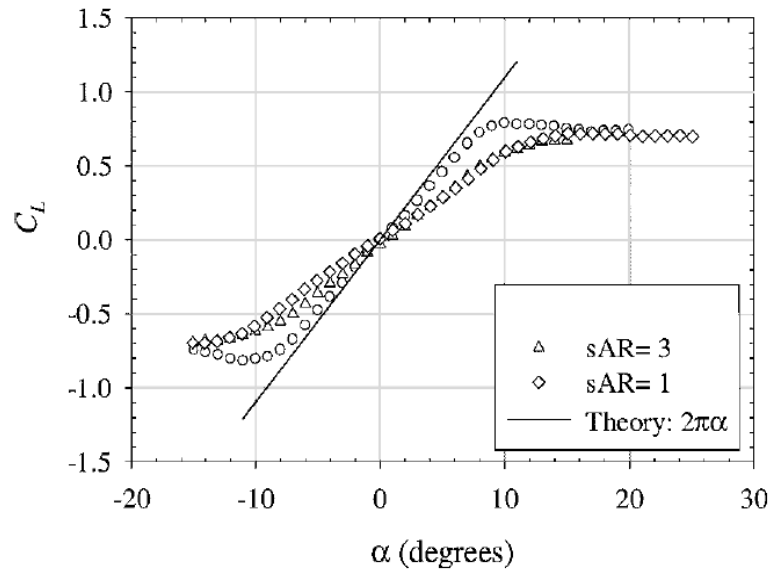


FIGURE 2.4: lift coefficient Vs. Angle of attack [17]

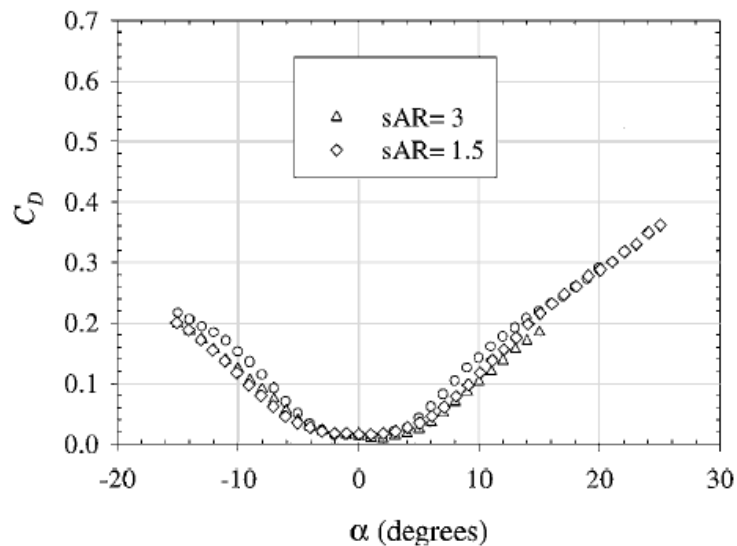


FIGURE 2.5: drag coefficient Vs. Angle of attack [17]

In the University of Colorado, Boulder, the final design of the MAV was a fixed wing puller prop aircraft. The motor, propeller, battery, speed controller, radio control receiver and servos are all hobby products. The camera and video transmitter are made for home surveillance. The fuselage and airframe are made of carbon fiber, fiberglass, MonoKote and balsa wood. The components are arranged to attain a center of gravity at the quarter cord of the center of the wing. The weight of the MAV was 67.2 grams. Tests were performed for a range of angles of attack at

the flight velocity of 15.5 m/s and also for a range of velocities at the flight angle of attack of 8°. These tests were completed and data was gathered for the lift and drag forces as well as the pitching moment. The results were then compared to the analytical results calculated by XFLR5 and AVL to obtain an estimate of the error associated with using conventional aircraft design tools to design a micro air vehicle. The experimental results were also compared to the results of the X-Wing software being developed at the University of Colorado to validate the software. However details of methodology used and results are not shown in this journal. [18]

Unmanned Aerial vehicles (UAVs) can be characterized and classified in different ways, such as flight altitude, endurance, observability, size, etc. Some attempts have been made to group them into Tiers, but there is such a variety of vehicles that there are always some that overlap the categories. The UAV Forum has descriptors for UAVs based on flight envelope, size/weight and function. [19]

Category	Designation	Max Alt	Radius	Speed	Endurance	Example
Tier I	Interim-Medium Altitude, Endurance	Up to 15,000 ft	Up to 250 km	60-100 kn	5-24 hrs	Pioneer; Searcher
Tier II	Medium Altitude, Endurance	3,000 ft to 25,000 ft	900 km	70 kn cruise	More than 24 hrs	Predator (used in Bosnia)
Tier II Plus	High Altitude, Endurance	65,000 ft max	Up to 5,000 km	350 kts cruise	Up to 42 hrs	Global Hawk
Tier III Minus	Low Observable - High Altitude, Endurance	45,000 ft to 65,000 ft	800 km	300 kn cruise	Up to 12 hrs	Darkstar

Figure 2.8: UAV Tier Classification and Characteristics [19]

In Venezuela, an UAV is designed for the purpose of petroleum exploration. It is called ANCE. It uses a rectangular wing with 0.254 span and 0.052m chord NACA airfoil. The aerodynamic characteristics of the initial design are being improved, by making modifications in the land gear and the wing tips. The methods used airfoil analysis computational code visual foil is used and experimental testing by using wind tunnel testing. Polar curves of design were traced. From the

modification made, efficiency was increased by 6% by experimental method and 16% by theoretical methods. [20]

In the journal of “Reverse Engineering and Aerodynamic Analysis of a Flying Wing UAV”. The UAV given is basically a flying wing but with a central fuselage that follows the reflex airfoil shape longitudinally and adapts to the curved ‘M’ shaped, tip to tip wing layout when viewed from the back. The entire aircraft (modular wings and fuselage) is constructed using ultra-light weight composite Kevlar fiber. Its fuselage is specifically designed to house 4 Lithium batteries, a speed controller and a rear pusher propeller unit. The craft is estimated to be able to carry a payload of 1.5 kilograms and fly at speeds up to 20 m/s. effectively, there are only two control surfaces on the UAV. These are the left and right elevons found at the ends of the wings of the aircraft. These control the pitching and rolling on this UAV. The wing could not be matched with any available wing in NACA airfoils, so they had to generate a full 3-D CAD model. By using the Minolta, VIVID 900, Non-Contact-3D Digitizer Image Laser scanner the photographed the entire wing profile and fuselage with a tolerance of ± 1.5 mm. The model was then sectioned and sliced at critical intervals to obtain the exact structural coordinates to be used to design and construct the wings. The entire CAD model was also imported into GAMBIT, and modified to avoid any skewed edges before generating FLUENT compatible 3D surface and volumetric meshes. [21]

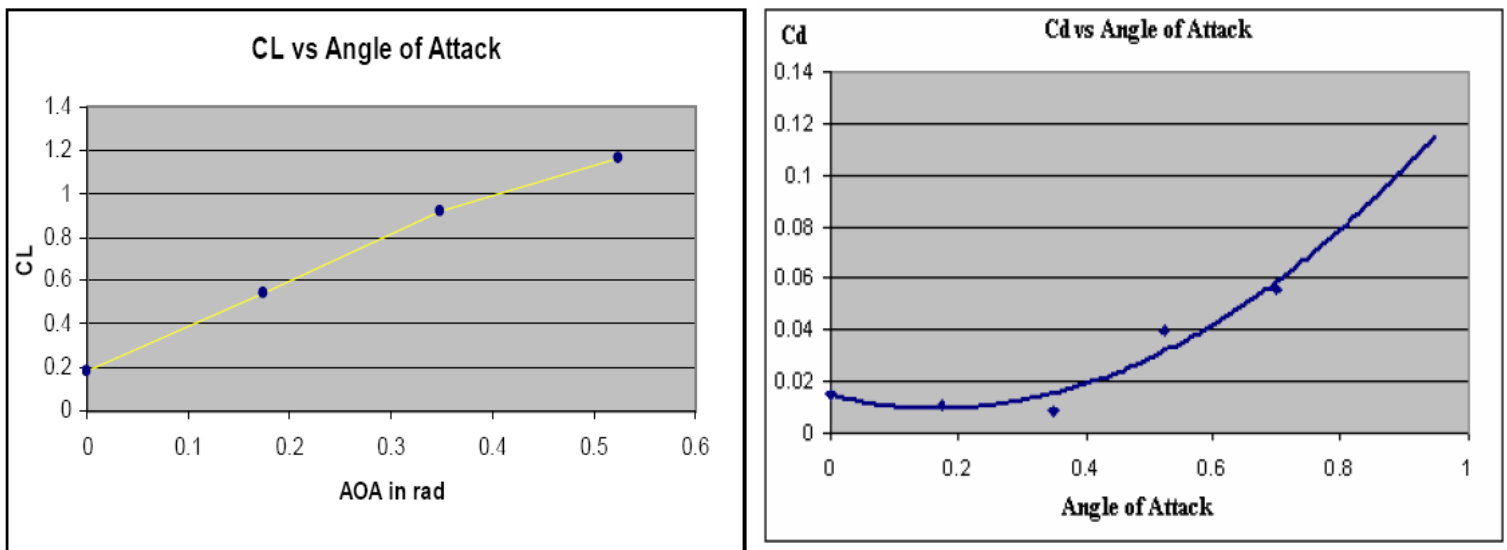


FIGURE 2.6: lift and drag coefficients vs. angle of attack [21]

From the journal of “High altitude long endurance unmanned aerial vehicle of a new generation” This paper describes a design process of HALE PW-114 sensor-craft, developed for high altitude (20 km) long endurance (40 h) surveillance missions. Wing control surfaces provide longitudinal balance. Fin in the rear fuselage section together with wingtips provide directional stability. Airplane is equipped with retractable landing gear with controlled front leg that allows operations from conventional airfields. According to the initial requirements it is twin engine configuration; typical payload consists of electro-optical/infra-red FLIR, big SAR (synthetic aperture radar) and SATCOM antenna required for the longest range. Tailless architecture was based on both Horten and Northrop design experience. Global Hawk was considered as a reference point.

Parameter	Requirement	Extreme value(s)
Altitude	60 000ft on loiter	65 000 ft
Flight speed	Mach 0.6 at loiter alt.	max Mach number: 0.65 due to aerodynamic efficiency (dramatically increase of wave drag on airfoils)
Endurance	24 h on loiter	Min 8 h
Range	1000 km	200-1000 km
Take off & landing	Use of conventional airports	
Payload weight	500 kg	Min 350 kg
Power tapping	8 kW	
Climb performance	55 000 ft reached in 30 min	Less than 1 hour
Payload volume or dimensions (Length × width × height)	Sensor equipment area (several racks) : 0.5 m ³ SAR antenna : 1.1 m × 0.5 m × 0.3 m EO/IR sense part: 1 m × 0.7 m × 0.7 m	0.4 to 0.6 m ³ - Racks (units) dimensions are typically 0.5 m × 0.5 m × 0.5 m Max SAR antenna: 2.5 m × 0.6 m × 0.5 m
Communication	SATCOM antenna volume: sphere of 1.0 m diameter	The use of SATCOM antenna depends on range

Figure 2.7: Requirements developed for BWB HALE aircraft [22]

HALE PW-114 main geometric data. Reference wing area 44.38 m², Span 28 m, Aspect ratio 17.7, MAC (Mean Aerodynamic Chord) 2.02 m, Wing taper ratio 0.355, Wing average thickness t/c 17.5%, Fuselage length 6.95 m, Wetted area breakdown: Wing 75.57 m², Body 22.82 m², Nacelle 13.68 m² Vertical stabilizer 7.81 m², Total 119.88 m², Wing airfoil definition LRT-17.5, Tail airfoil definition NACA 0015. [22]

In the University of Sydney “school of aerospace”. The Brumby Mk I is the first version of the Brumby and, as an indication of the success of rapid prototyping; it was built in less than six weeks (including the fabrication of tooling and composite moulds). First flight was on 21 November 1997. It was demonstrated to be a stable flight platform well suited to research requiring the carriage of sensors on a flight platform. The maximum takeoff weight of the Brumby Mk I was of 30kg, its maximum endurance was of approximately 30 minutes, and achieved a maximum speed in excess of 51.44 m/s. A wind tunnel model was subsequently built and tested in the department’s 4x3 Low Speed wind tunnel. After all the success of the Brumby Mk I, it was decided to build an upgraded version of the Brumby. The new version is called Brumby Mk II and has the same basic configuration of the Mk I. The Brumby Mk II incorporated several significant changes. The wing plan form area was increased, with slight increases in span (almost half a meter) and reduction in sweep. The aerofoil section was changed from the original NACA 0010 section to that of a modified S1012 section. [23]

The MAV40 is a delta-wing aircraft; it has a wingspan of 40 cm, an aspect ratio of 1.8 and a total weight of 252 g including sensors, actuators and communication systems. The sensor interface is composed of angular rate sensors, accelerometers, pressure sensors, altimeter, GPS system, all of which are integrated in an Inertial Measurement Unit (IMU). The IMU (O-NAVI Phoenix) was programmed using GNU tools for MCore. The MAV40 has three inputs, two elevons and one Electrical propeller. Elevons are deflection surfaces and have a direct influence on the aerodynamic forces. They can behave as elevators or ailerons at the same time, resulting in two different inputs, elevator deflection (δ_e) and aileron deflection (δ_a), both of them with unit in radian. Two servomotors act as actuators for the elevons. [24]

After months of researches and literature review, it was found that the most important factor for a flight is lift. After going through journals and paper it was found out through graphs, at a certain angle of attack after the lift coefficient starts to decrease after being increasing and that occurs due to stall.

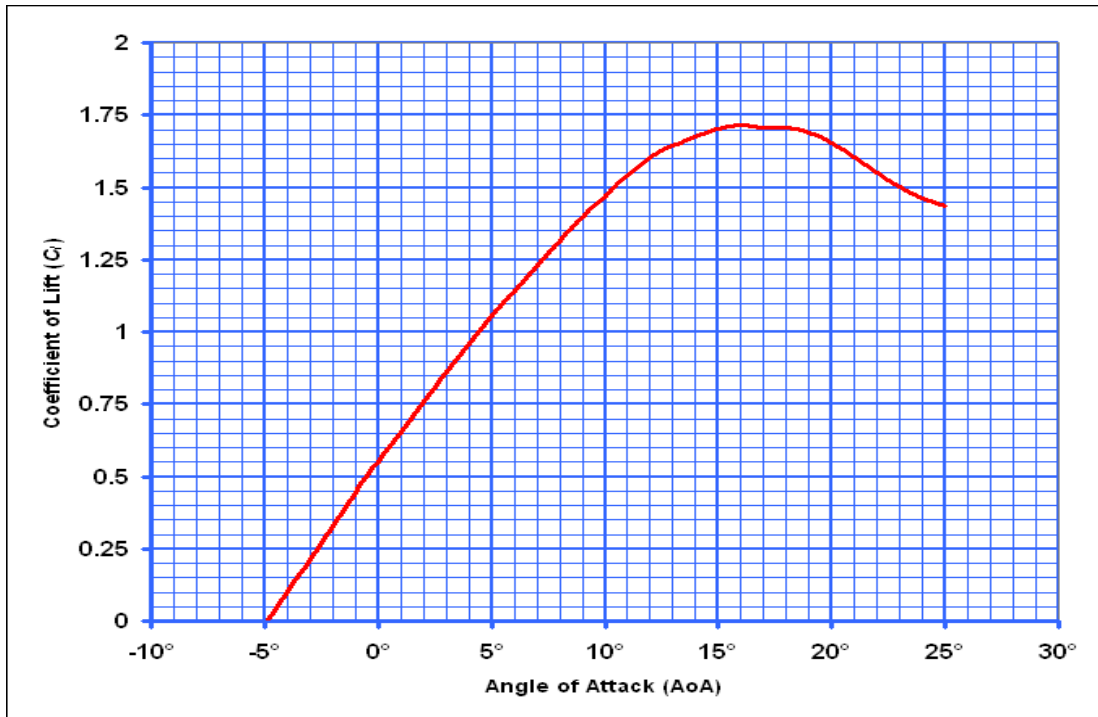


FIGURE 4.1: coefficient of lift vs. angle of attack [16]

From the upper graph it is clear that after the lift coefficient increased to 1.7 at an angle of attack of 15° it started to decrease again and that is due to stall.

Stalls depend only on angle of attack, not airspeed. However, a correlation with airspeed exists. And so, a "stall speed" is usually used in practice. It is the speed below which the airplane cannot create enough lift to sustain the weight in 1g flight. In steady, level flight (1g), the faster an airplane goes the less angle of attack it needs to hold the airplane up. As the airplane slows down, it needs to increase angle of attack to create the same lift. As the speed slows further, at some point the angle of attack will be equal to the critical (stall) angle of attack. This speed is called the "stall speed". The angle of attack cannot be increased to get more lift at this point and so slowing below the stall speed will result in a descent. And so, airspeed is often used as an indirect indicator of approaching stall conditions. The stall speed will vary depending on the airplane's weight and configuration. [25]

One way of overcoming stall for an airplane is using a camber wing.

Camber is often added to an airfoil to increase lift and/or reduce the critical angle of attack (the angle at which the airfoil begins to stall). The camber of a wing may vary from wing root to wing tip

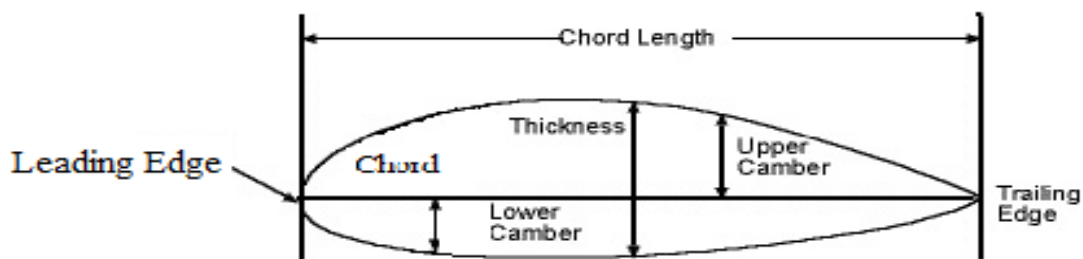


FIGURE 4.2: airfoil with camber [26]

Adding camber doesn't necessarily increase lift; it depends on the airfoil shape. If too much camber is added, the flow over the airfoil may not stay attached to the wing even at an angle of attack of zero. When this occurs, we say the flow has separation over the airfoil, if the entire top of the wing has separation, the wing is stalled. Wings with camber don't as a result have the ability to produce more lift in general. Cambered wings will produce lift at zero angle of attack, but as mentioned, too much camber can also be a bad thing.

In the journal of "Development of a small air vehicle based on aerodynamic model analysis in the tunnel tests" Muller et al designed and built a new plan form with force and moment balance to perform lift, drag and moment measurements on small air models at the low Reynolds numbers. Moreover, it was found that the cambered-plate wings with 4% camber offer better aerodynamics characteristics than flat-plate wings at given Reynolds numbers. [27]

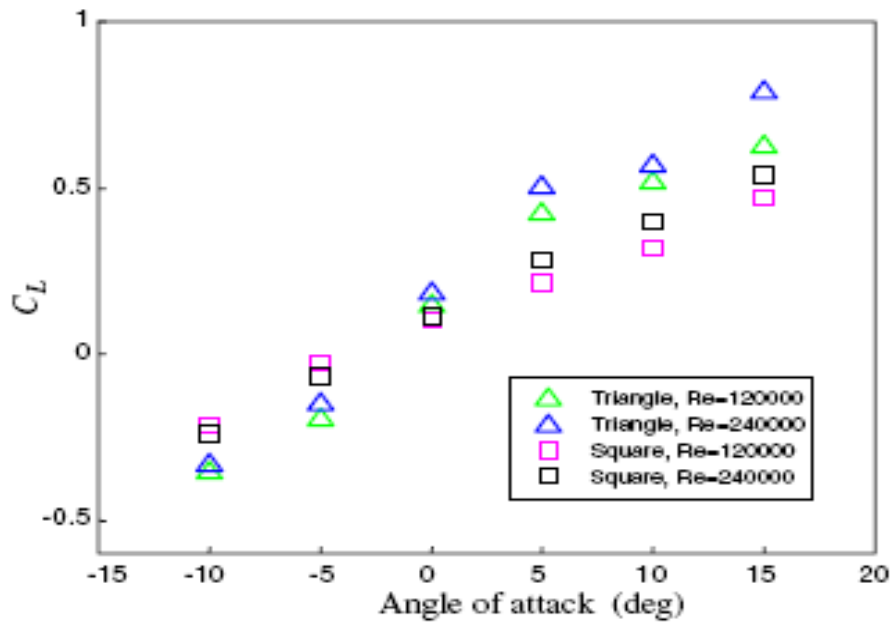


FIGURE 4.3: coefficient of lift vs. angle of attack [28]

From the upper graph it is clear that after an angle of attack of 15° the lift is still increasing with an airfoil of 4% camber.

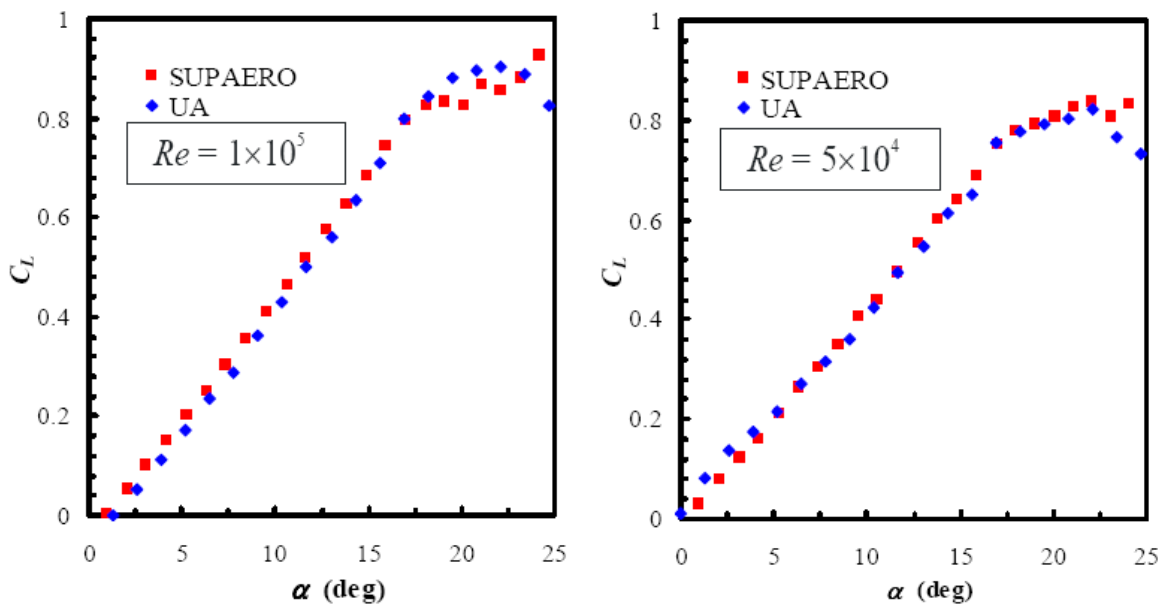


FIGURE 4.4: coefficient of lift vs. angle of attack with different Re numbers [29]

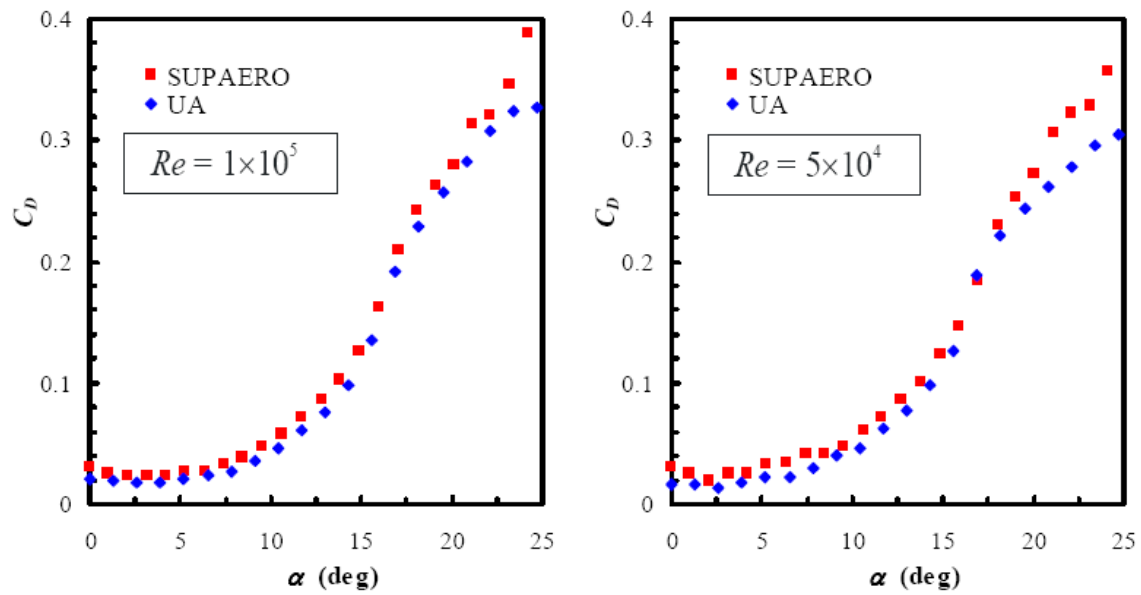
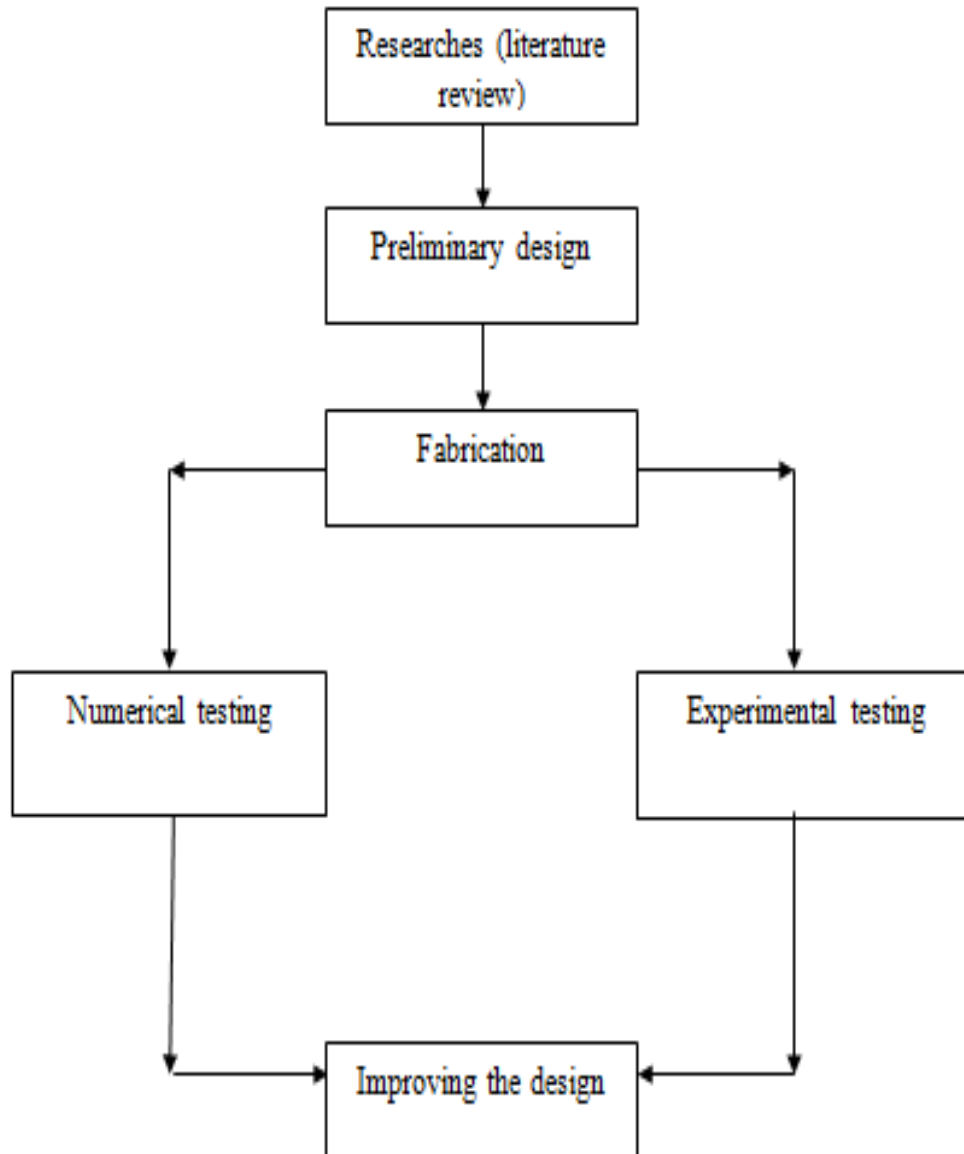


FIGURE 4.5: coefficient of drag vs. angle of attack with different Re numbers [29]

From the all the graphs shown in this report it is clear that the lift coefficients of the unmanned aerial vehicles all have precision values, so from these graphs it is quite obvious that for the models that is being designed should have the same result like the other unmanned vehicles in the experimental testing (wind tunnel) in order to be a successful prototype.

CHAPTER 3

METHODOLOGY



The methodology for the final year project first part includes researches for better understanding (literature review) then a preliminary design will be done, computational testing should be carried out, fabrication of the prototype and last but not least experimental testing will be done using the wind tunnel available in the university.

3.1 RESEARCHES (LITERATURE REVIEW)

The literature review is about researching in the field of the project, by gathering as much information as possible. It is information that will build a strong background for the accomplishment of the project, it will help in understanding the aerodynamics characteristics and it will also help understanding the fundamentals of flight.

3.2 PRELIMINARY DESIGN

After the literature review, a simple design is supposed to be done according to the understanding from the researches.

3.3 COMPUTATIONAL TESTING

Testing will be carried out using computational fluid dynamics software, FLUENT. It is used for simulation, visualization, analysis of fluid flow, heat and mass transfer and in chemical reactions. Also software will be used, which is GAMBIT; it is used to allow creation of geometry or improving geometry from most CFD packages.

3.4 PROTOTYPE FABRICATION

This will also involve some researches on the most appropriate material, and methods of fabrication that will be done in order to make the prototype needed.

3.5 EXPERIMENTAL TESTING

Wind tunnel testing is used for testing lift, drag and angle of attack characteristics. The model of the UAV must fit the wind tunnel where the dimensions of the test section of 0.3m x 0.3m x 1.5m long. 3.6 improvements

3.6 IMPROVING

After the fabrication of the prototype wind tunnel testing will take place. After getting results from the wind tunnel, if the results are inaccurate improvements in the design has to be done in order to get accurate results.

3.7 Tools Required

In general, the one of the main task of this project is to design and fabricate an unmanned aerial vehicle which is smaller than the usual one, and can perform better. The tools below are required during the project completion.

1. Software

- AutoCAD
- FLUENT AND GAMBIT

2. Tools

- CNC machine
- Milling machine
- Lathe machine
- Wind tunnel

3.8 GANTT CHART

No.	Detail/ Week	1	2	3	4	5	6	7	8	9		10	11	12	13	14	
1	Project Work Continues	■	■	■							Mid-semester break						
2	Submission of Progress Report I				●												
3	Further Research on Case Study				■	■	■	■	■	■							
4	Submission of Progress Report II								●								
5	Seminar (compulsory)								●								
6	Project Work Continues												■	■	■	■	
7	Poster Exhibition												●				
8	Submission of Dissertation (Soft Bound)																●
9	Oral Presentation												During the study week				
10	Submission of Dissertation (Hard Bound)											After Oral Presentation by 7 days					

● Suggested Milestones

■ Process

CHAPTER 4

RESULTS AND DISCUSSION

4.1 DESCRIPTION OF THE OPEN CIRCUIT WIND TUNNEL

The main characteristics and capabilities of the wind tunnel are shown in the table below:

NO	Item	Specification
1.	Type of tunnel	WTO 4 subsonic wind tunnel system
2.	Mach number	0.1
3.	Test section	300H x 300W x 900L mm
4.	Overall dimension	1900H x 1400W x 6000L mm
5.	Max speed in the test section	70 m/s equal to 252 km/h
6.	Motor	AC/DC motor , adjustable speed.
7.	Power requirement	380 vac 50 Hz, 3 phase
8.	Material of construction	Acrylic sheet or laminated glass up on requested. The whole duct is supported by a basement in rectangular steel section.

Table 4.1: open circuit wind tunnel system

NO	Testing capabilities
1.	Study of air flow behavior through / around engineering models
2.	Lift and drag of aerofoils
3.	Pressure distribution measurement on the MAV or on other models

Table 4.2: wind tunnel experimental capabilities



Figure 4.1: UTP open-circuit wind tunnel

4.2 DESIGN OF AMSA MAV MODEL:

AMSA MAV was chosen as the best design to fabricate among to other two designs, the wings were changed to front curve shape. It has a curved front area to try and reduce the drag force as much as possible. The shape is shown in the following Figure

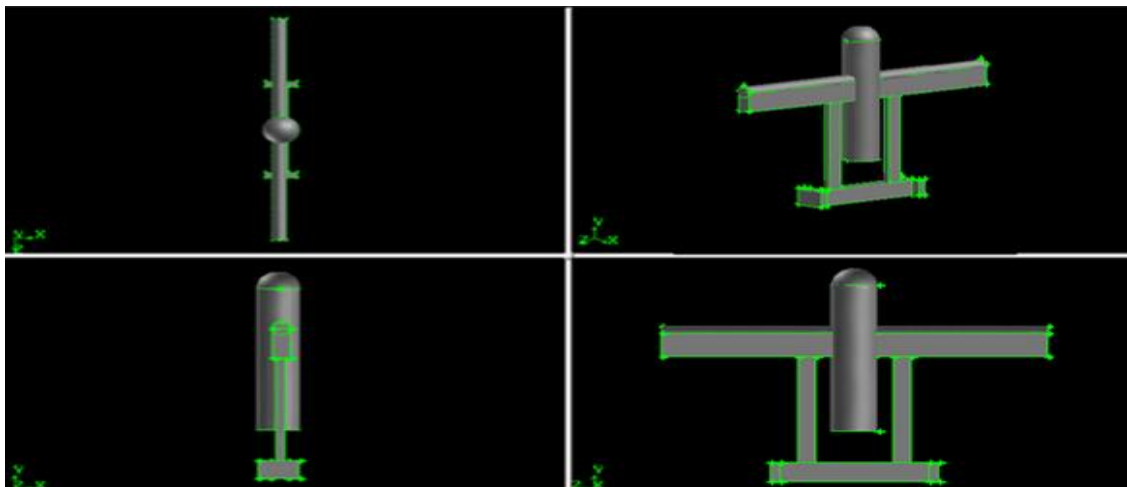


Figure 4.2: Four Views of MAV design

The design was made by using FLUENT and GAMBIT softwares, then the design was used in the AUTOCAD in order to get the coordinates of the design, as shown in the figure below:

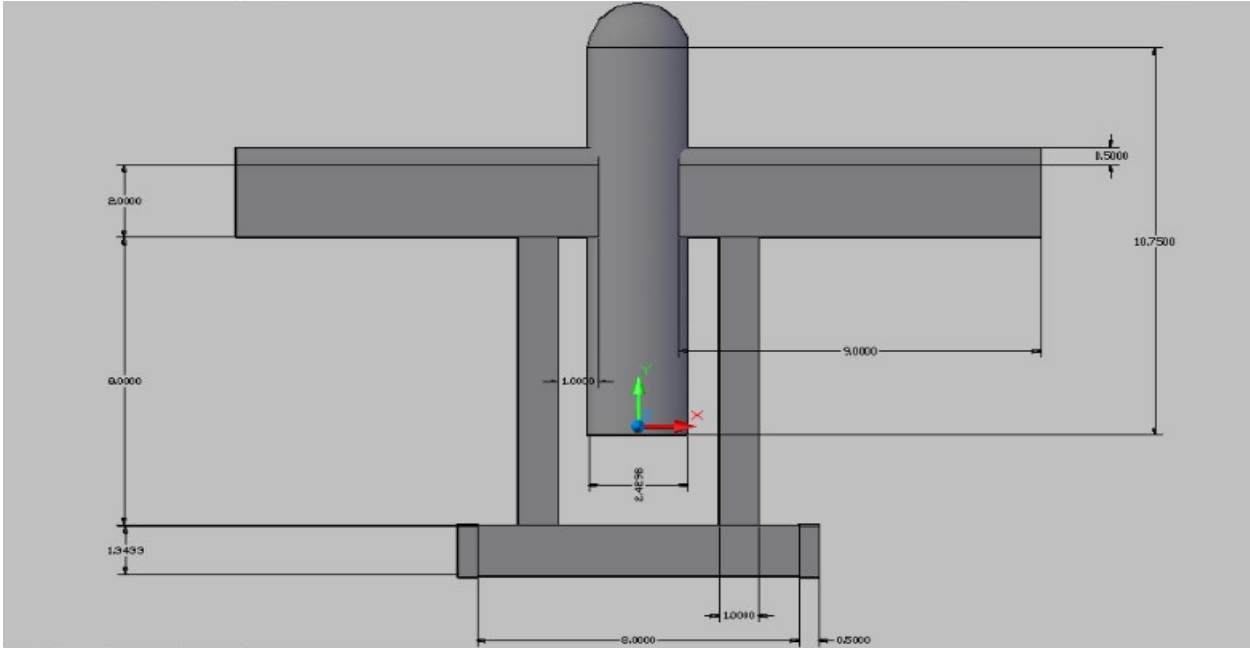


Figure 4.3: MAV design

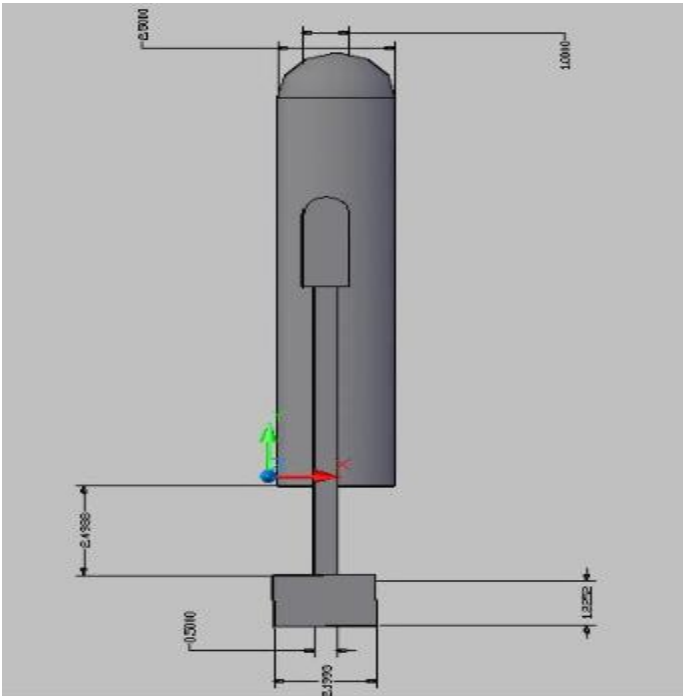


Figure 4.4: MAV design

4.3 FABRICATION OF AMSA MAV MODEL

The material used in the fabrication of the AMSA MAV was aluminium. The aluminium material is available in utp manufacturing labs. The problem with the aluminium blocks is that it was too big to be put in the CNC machine, so it was cut to smaller pieces using conventional milling machine to the specified dimensions.

After the aluminium blocks were cut, some parts were fabricated using CNC lathe and others were done by CNC milling. After fabricating each part separately, holes were drilled in them from the top and the bottom, and screws were put from the inside in order to attach all the parts together, and then these holes were covered using small round aluminium pieces.

In the part where the parts are being attached to each other, welding was not used in order to enhance the aerodynamics characteristics, because with welding the MAV will not have a good surface finish, it's well known that drag and lift are very sensitive in getting the readings, so any precipitation on the MAV, because the welding operations produce an isolation layer and it must be removed after finishing, which will ruin the aerodynamic design of the MAV.



Figure 4.5: CNC machine



Figure 4.6: welding process

Lastly, the complete model is shown in figure 4.7 and 4.8. the MAV is fixed in the wind tunnel test section during testing.

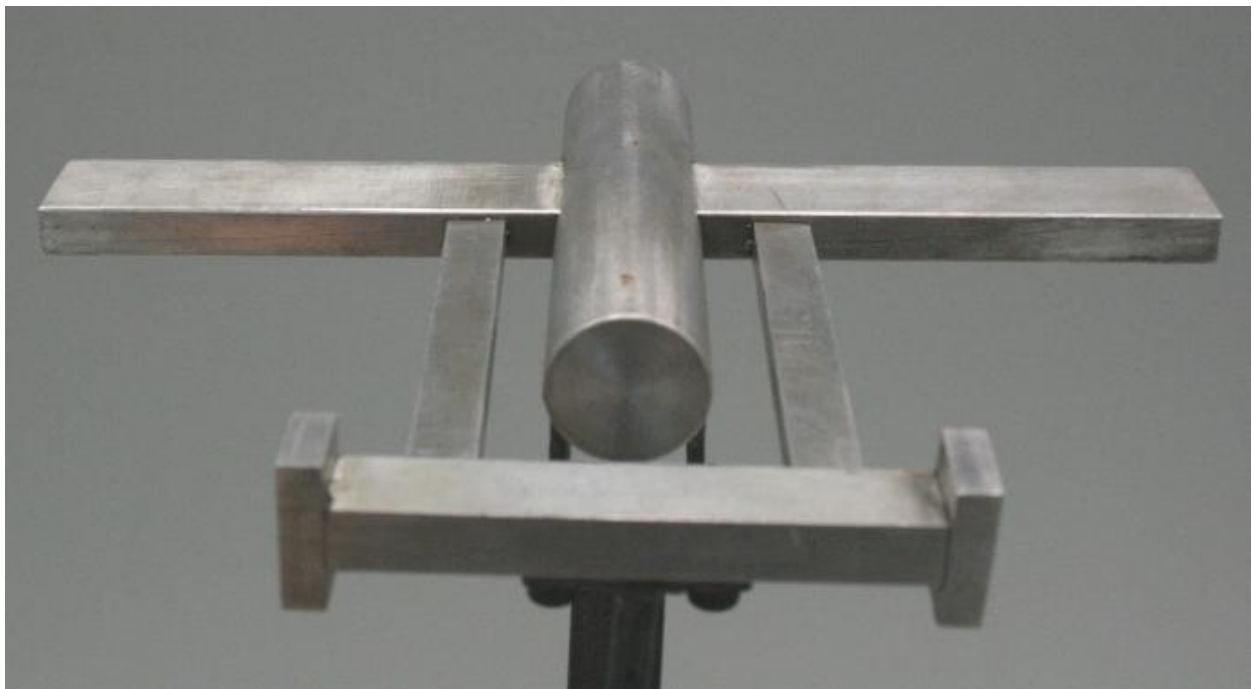


Figure 4.7: MAV model ready for the wind tunnel testing



Figure 4.8: MAV in the wind tunnel testing section

4.4 EXPERIMENTAL RESULTS AND ANALYSIS

4.4.1 Experimental results on the characteristics on coefficient of lift and coefficient of drag vs Angle of Attack.

The lift and drag forces are measured experimentally using the wind tunnel. The lift and drag forces are recorded for various velocities and various AOA, results are shown from table 4.1 to 4.8, while the lift and drag coefficient are calculated using equation 12, the results of both are also shown from table 4.1 to 4.8.

Angel of Attack	Lift force	Coefficient of lift	Drag force	Coefficient of
0	3.59	0.009719	1.33	0.003601
1	3.98	0.010775	1.87	0.005063
2	4.11	0.011127	1.92	0.005198
3	4.43	0.011993	1.53	0.004142
4	4.64	0.012562	0.91	0.002464
5	8.95	0.02423	2	0.005415
6	8.96	0.024257	5.89	0.015946
7	9.22	0.024961	0.89	0.002409
8	9.33	0.025259	0.21	0.000569
9	10.26	0.027777	-0.64	-0.00173
10	10.74	0.029076	3.21	0.00869
11	11.23	0.030403	1.43	0.003871
12	11.45	0.030998	3.53	0.009557
13	12.79	0.034626	3.28	0.00888
14	13.03	0.035276	4.09	0.011073
15	15.29	0.041394	1.4	0.00379
16	16.67	0.04513	2.5	0.006768
17	6.3	0.017056	1.04	0.002816
18	9.06	0.024528	1.77	0.004792
19	8.96	0.024257	2.26	0.006118
20	9.69	0.026234	3.34	0.009042

Table 4.3: coefficient of lift & drag at 25 m/s

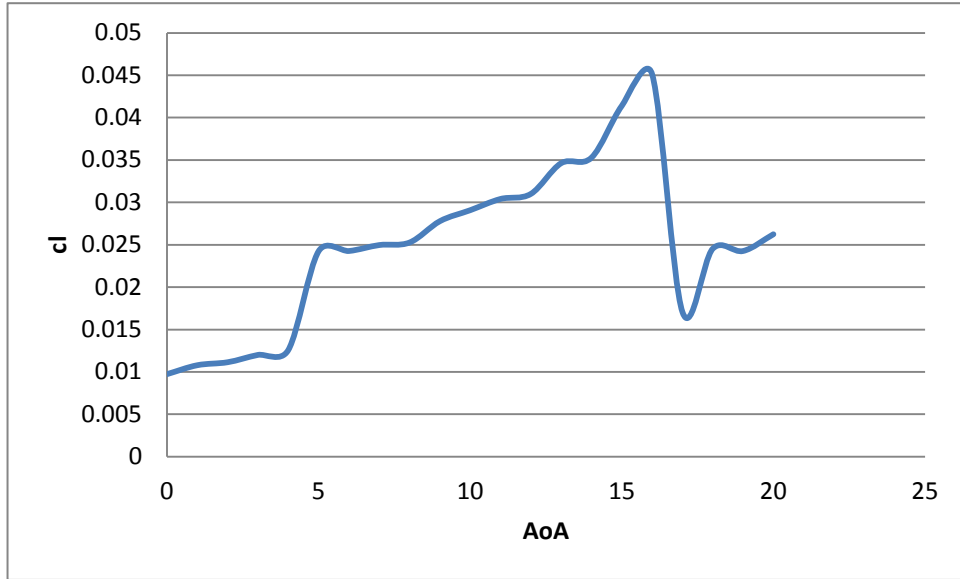


Figure 4.9: coefficient of lift vs AOA at 25 m/s

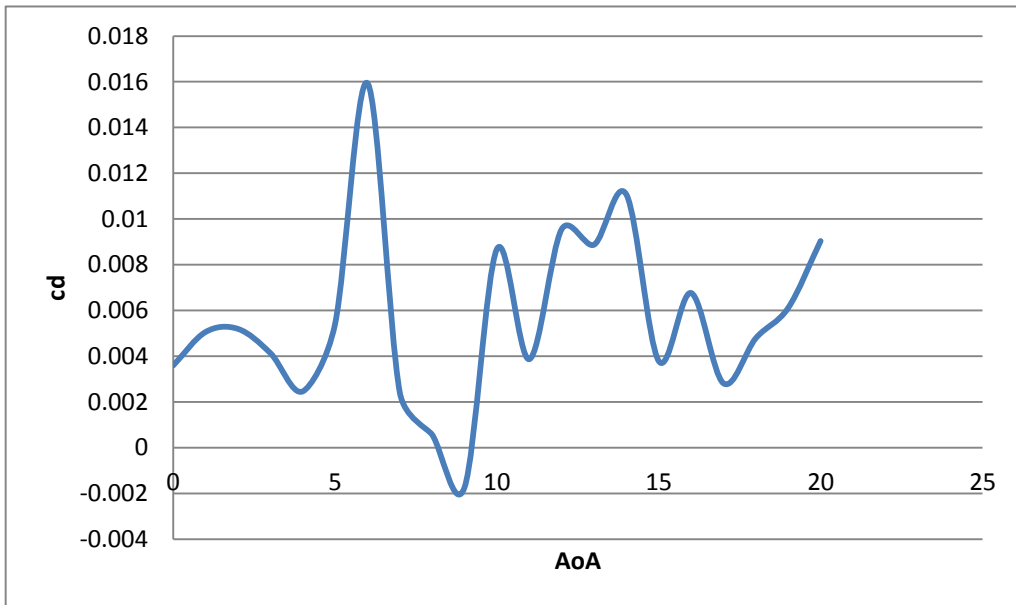


Figure 4.10: coefficient of drag vs AOA at 25 m/s

Angel of Attack (degree)	Lift force	Coefficient of lift	Drag force	Coefficient of drag
0	4.32	0.008122	1.92	0.00361
1	3.91	0.007351	2	0.00376
2	5.83	0.010961	2.47	0.004644
3	4.69	0.008817	2.36	0.004437
4	6.04	0.011356	1.77	0.003328
5	9.3	0.017484	2.87	0.005396
6	9.49	0.017842	6.7	0.012596
7	10.43	0.019609	1.26	0.002369
8	11.87	0.022316	0.79	0.001485
9	12.4	0.023313	0.7	0.001316
10	12.87	0.024196	3.72	0.006994
11	13.38	0.025155	3.77	0.007088
12	13.68	0.025719	4.75	0.00893
13	14.03	0.026377	4.04	0.007595
14	15.7	0.029517	5.55	0.010434
15	16.88	0.031735	3.28	0.006167
16	16.89	0.031754	4.66	0.008761
17	7.9	0.014852	2.77	0.005208
18	11.25	0.021151	2.79	0.005245
19	12.66	0.023801	3.4	0.006392
20	12.85	0.024159	4.23	0.007953

Table 4.4: coefficient of lift & drag at 30 m/s

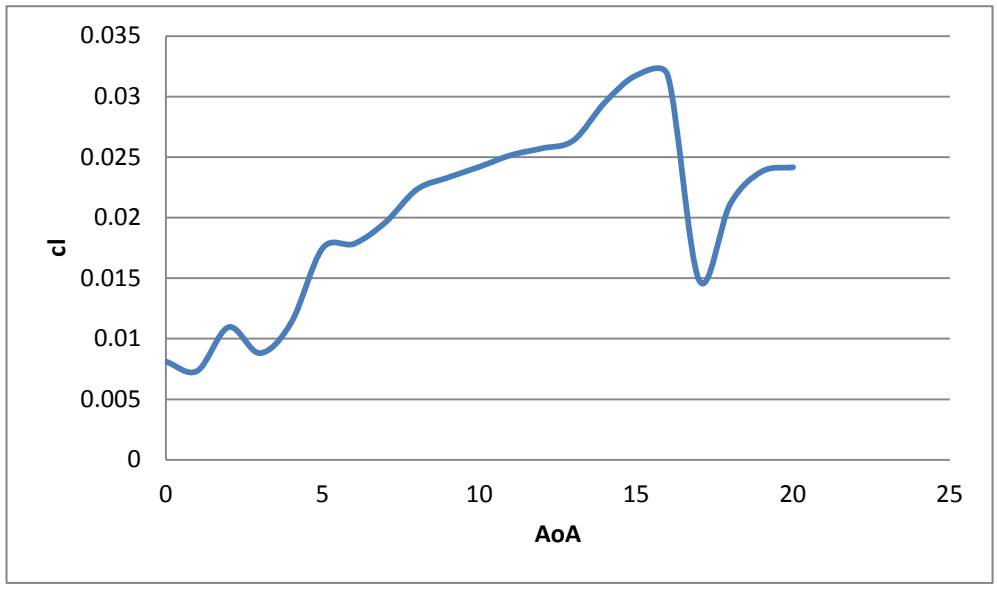


Figure 4.11: coefficient of lift vs AOA at 30 m/s

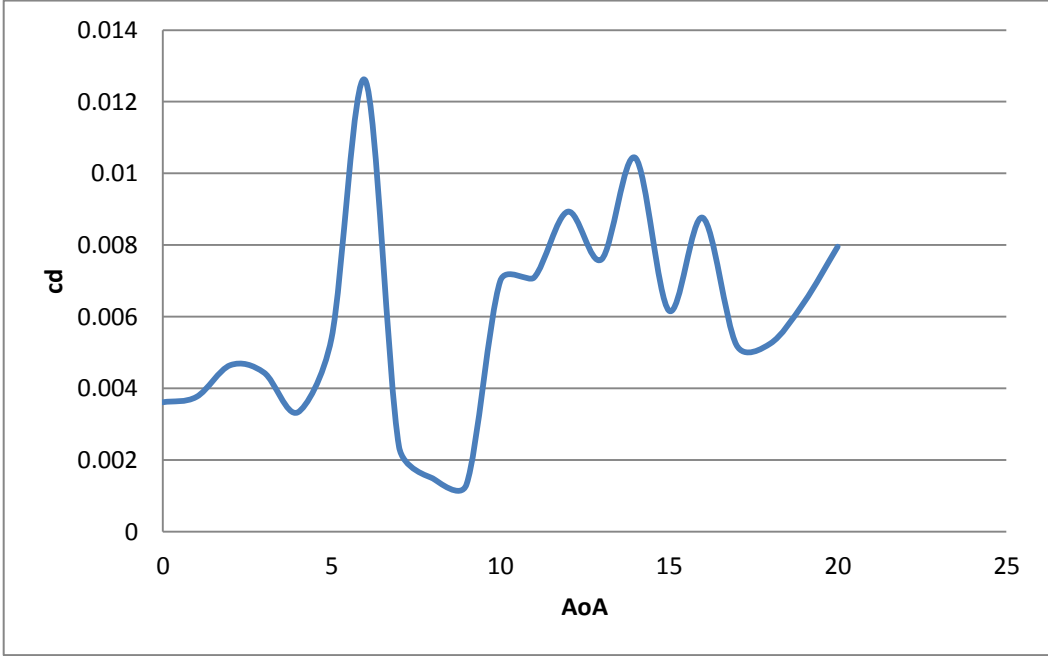


Figure 4.12: coefficient of drag vs AOA at 30 m/s

Angle of Attack (degree)	Lift force	Coefficient of lift	Drag force	Coefficient of drag
0	5	0.006906	2.21	0.003053
1	4.9	0.006768	2.43	0.003356
2	5.89	0.008136	2.87	0.003964
3	6.2	0.008564	3.75	0.00518
4	7.08	0.009779	2.49	0.003439
5	7.39	0.010208	3.5	0.004834
6	8.21	0.01134	7.28	0.010056
7	9.01	0.012445	1.75	0.002417
8	10.63	0.014683	2.09	0.002887
9	12.78	0.017653	1.55	0.002141
10	13.1	0.018095	5.55	0.007666
11	11.24	0.015525	5.36	0.007404
12	11.72	0.016188	6.7	0.009254
13	12.38	0.0171	6.23	0.008605
14	12.99	0.017943	7.21	0.009959
15	16.15	0.022307	6.15	0.008495
16	18.78	0.02594	6.15	0.008495
17	8.7	0.012017	3.92	0.005415
18	11.3	0.015608	4.49	0.006202
19	12.92	0.017846	5.26	0.007265
20	13.26	0.018316	5.87	0.008108

Table 4.5: coefficient of lift & drag at 35 m/s

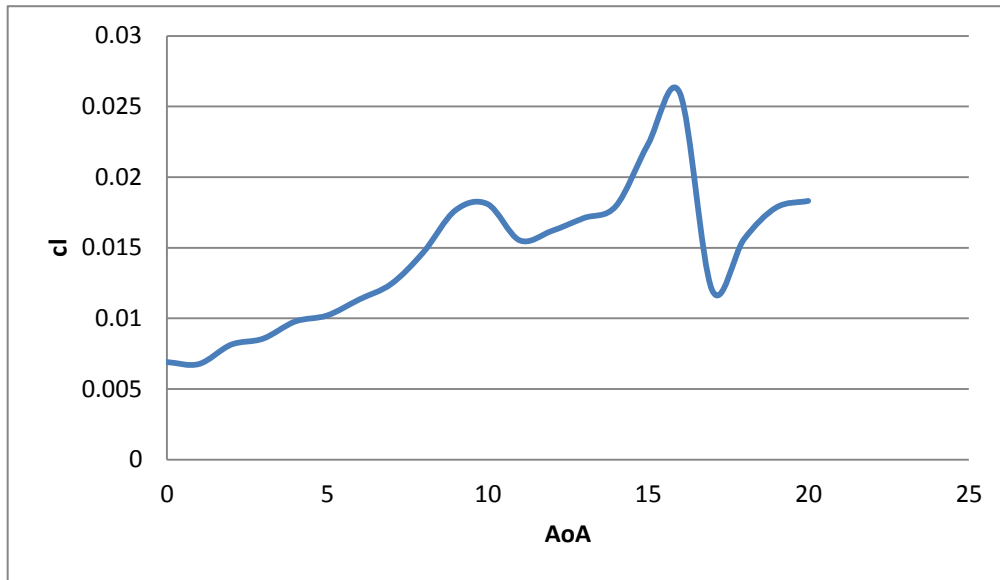


Figure 4.13: coefficient of lift vs AOA at 35 m/s

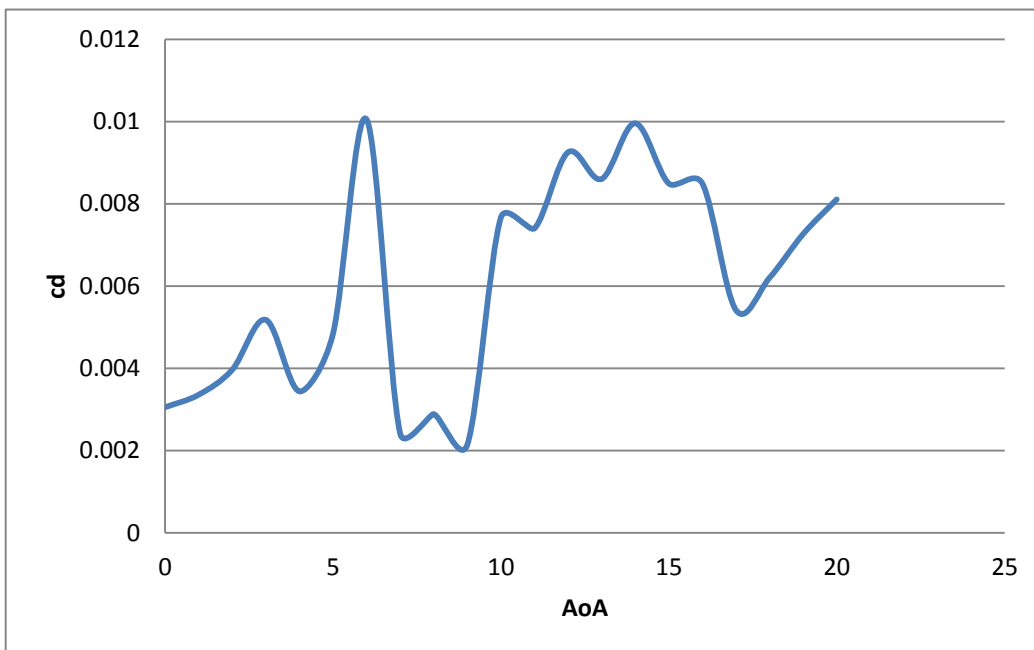


Figure 4.14: coefficient of drag vs AOA at 35 m/s

Angel of Attack (degree)	Lift force	Coefficient of lift	Drag force	Coefficient of drag
0	5.36	0.005668	3.49	0.003691
1	5.4	0.005711	3.6	0.003807
2	6	0.006345	3.95	0.004177
3	6.54	0.006916	4.26	0.004505
4	6.72	0.007107	4.06	0.004294
5	7.08	0.007487	5.7	0.006028
6	7.99	0.00845	8.38	0.008862
7	8.45	0.008936	3.49	0.003691
8	8.89	0.009401	4.11	0.004346
9	9.59	0.010142	3.3	0.00349
10	9.99	0.010565	6.91	0.007308
11	9.48	0.010025	8.15	0.008619
12	10.75	0.011368	8.5	0.008989
13	11.6	0.012267	8.79	0.009296
14	12	0.01269	9.43	0.009973
15	18.54	0.019607	7.6	0.008037
16	18.7	0.019776	9.3	0.009835
17	8.85	0.009359	5.32	0.005626
18	10.38	0.010977	6.7	0.007085
19	11.82	0.0125	7.64	0.00808
20	12.43	0.013145	8.01	0.008471

Table 4.6: coefficient of lift & drag at 40 m/s

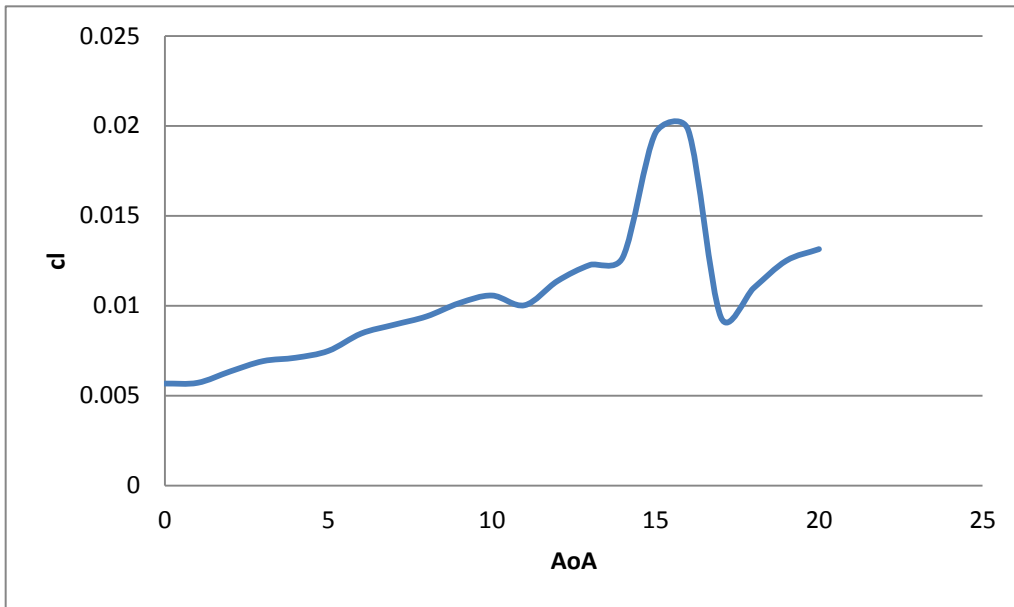


Figure 4.15: coefficient of lift vs AOA at 40 m/s

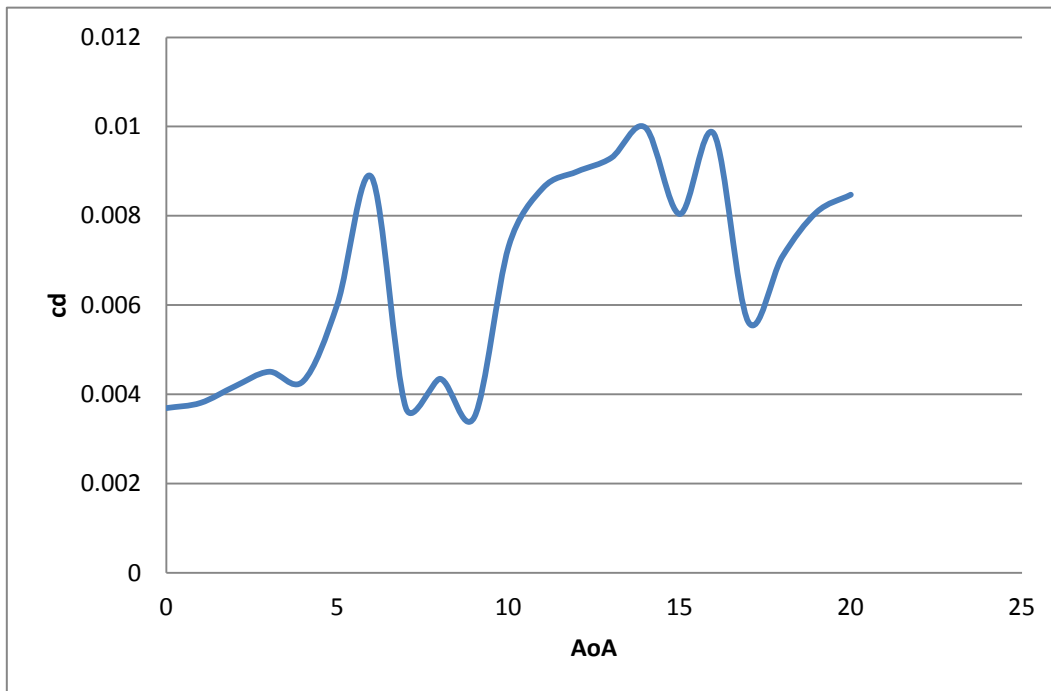


Figure 4.16: coefficient of drag vs AOA at 40 m/s

Angle of attack (degree)	Lift force	Coefficient of lift	Drag force	Coefficient of drag
0	4.53	0.003785	4.17	0.003484
1	5.69	0.004754	4.43	0.003702
2	6.51	0.00544	4.5	0.00376
3	7.03	0.005874	5.53	0.004621
4	7.4	0.006183	4.72	0.003944
5	7.52	0.006284	6.74	0.005632
6	7.7	0.006434	9.81	0.008197
7	7.91	0.006609	4.79	0.004002
8	10.99	0.009183	5.57	0.004654
9	11.72	0.009793	5.06	0.004228
10	12.21	0.010202	9.11	0.007612
11	10.99	0.009183	10.04	0.008389
12	12.02	0.010044	10.55	0.008815
13	13.26	0.01108	10.53	0.008799
14	13.72	0.011464	11.01	0.0092
15	14.22	0.011882	11.45	0.009567
16	16.25	0.013578	10.19	0.008515
17	9.32	0.007788	6.7	0.005598
18	11.04	0.009225	8.49	0.007094
19	11.46	0.009576	9.34	0.007804
20	12.79	0.010687	9.87	0.008247

Table 4.7: coefficient of lift & drag at 45 m/s

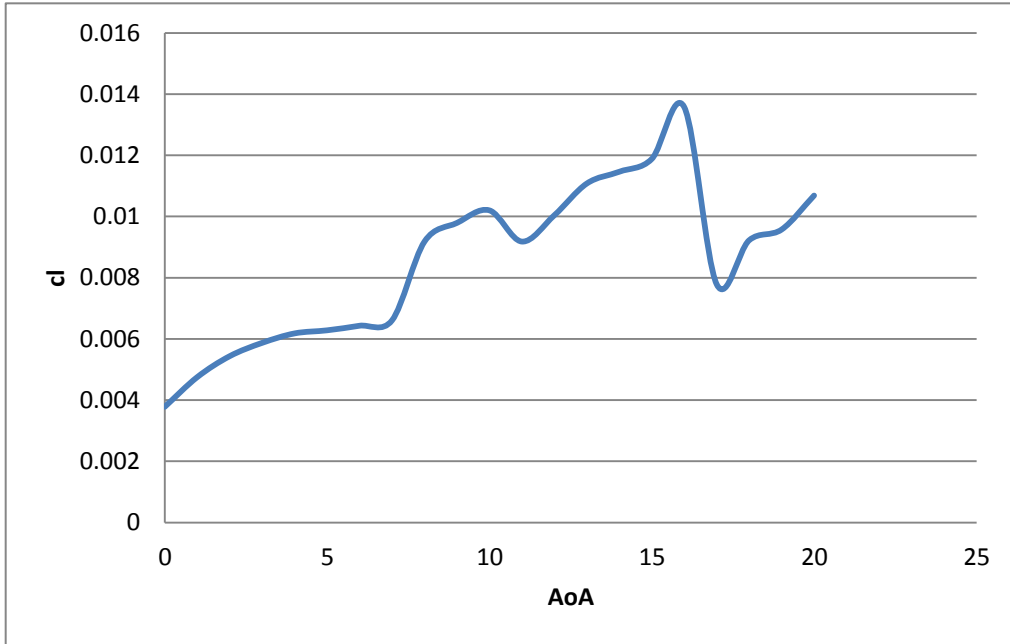


Figure 4.17: coefficient of lift vs AOA at 45 m/s

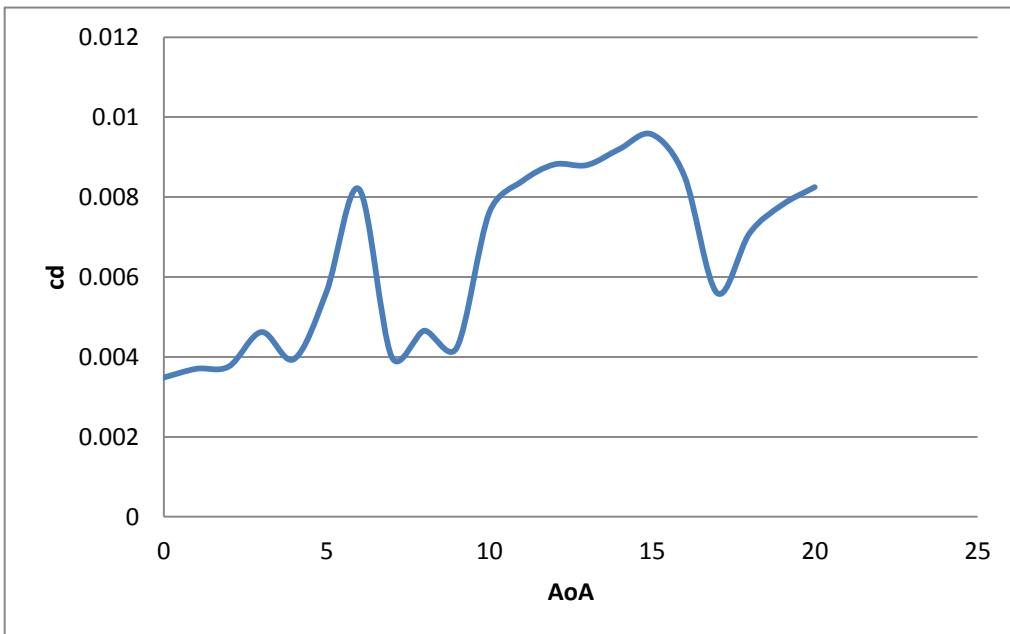


Figure 4.18: coefficient of drag vs AOA at 45 m/s

Angle of Attack (degree)	Lift force	Coefficient of lift	Drag force	Coefficient of drag
0	6.51	0.004406	5.08	0.003438
1	6.79	0.004596	5.15	0.003486
2	7.3	0.004941	5.57	0.00377
3	6.3	0.004264	6.7	0.004535
4	7.66	0.005184	6.23	0.004217
5	7.71	0.005218	8.23	0.00557
6	7.97	0.005394	12.13	0.00821
7	8.23	0.00557	5.87	0.003973
8	8.7	0.005888	7.72	0.005225
9	9.11	0.006166	6.99	0.004731
10	11.09	0.007506	10.6	0.007174
11	11.42	0.007729	12.21	0.008264
12	12.97	0.008778	13.51	0.009144
13	14.29	0.009672	14.4	0.009746
14	14.82	0.01003	14.56	0.009854
15	15.94	0.010788	13.89	0.009401
16	21.3	0.014416	15.81	0.010701
17	10.63	0.007195	10.19	0.006897
18	11.94	0.008081	11.83	0.008007
19	11.61	0.007858	12.25	0.008291
20	13.76	0.009313	13.55	0.009171

Table 4.8: coefficient of lift & drag at 50 m/s

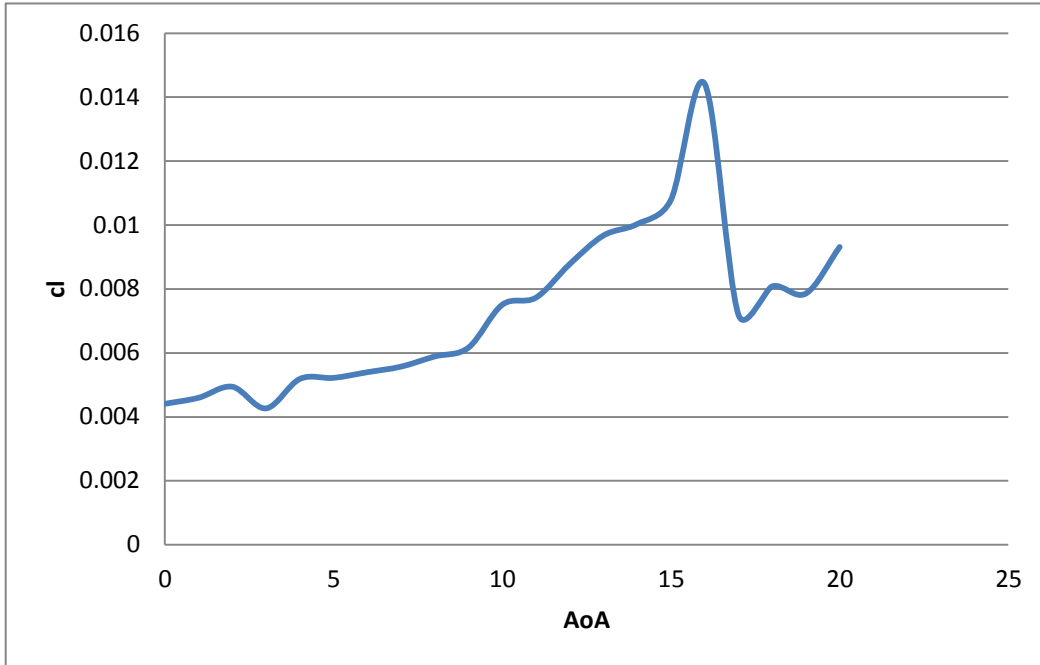


Figure 4.19: coefficient of lift vs AOA at 50 m/s

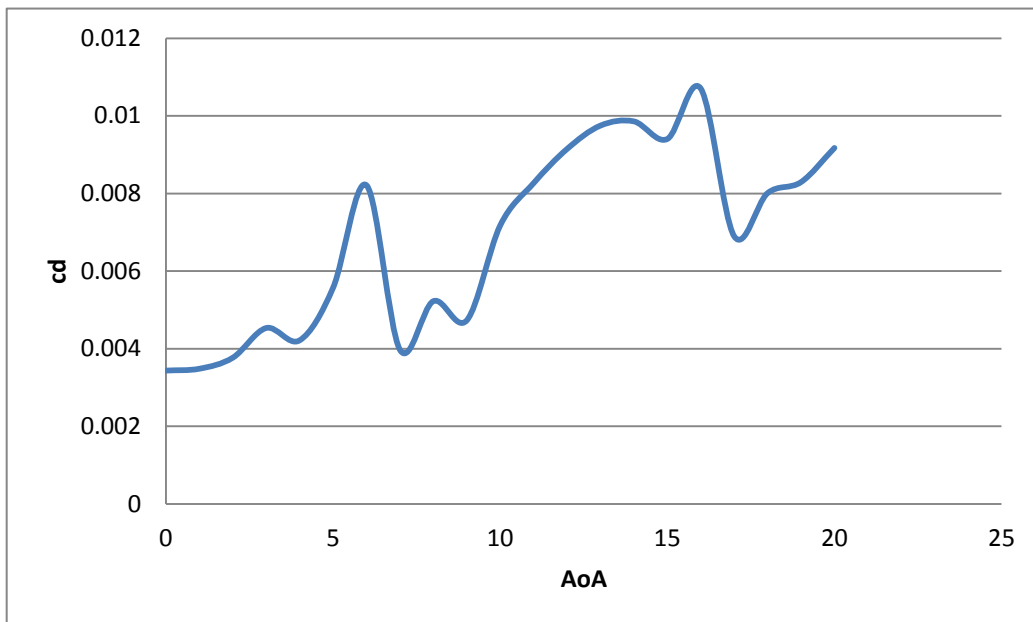


Figure 4.20: coefficient of drag vs AOA at 50 m/s

Angle of attack (degree)	Lift force	Coefficient of lift	Drag force	Coefficient of drag
0	6.54	0.003658	6.23	0.003485
1	6.82	0.003815	6.6	0.003485
2	7.75	0.004335	6.75	0.003485
3	8.49	0.004749	7.81	0.003485
4	9.49	0.005308	6.51	0.003485
5	9.75	0.005454	8.6	0.003485
6	10.99	0.006147	13.34	0.003485
7	11.75	0.006572	6.06	0.003485
8	12.98	0.00726	6.62	0.003485
9	13.48	0.00754	7.85	0.003485
10	14.11	0.007892	12.11	0.003485
11	11.98	0.006701	12.85	0.003485
12	13.39	0.00749	14.98	0.003485
13	15.36	0.008592	12.53	0.003485
14	15.39	0.008608	14.97	0.003485
15	17.29	0.009671	14.58	0.003485
16	19.53	0.010924	16.3	0.003485
17	12.24	0.006846	10.91	0.003485
18	13.28	0.007428	11.13	0.003485
19	14.27	0.007982	12.11	0.003485
20	14.56	0.008144	13.99	0.003485

Table 4.9: coefficient of lift & drag at 55 m/s

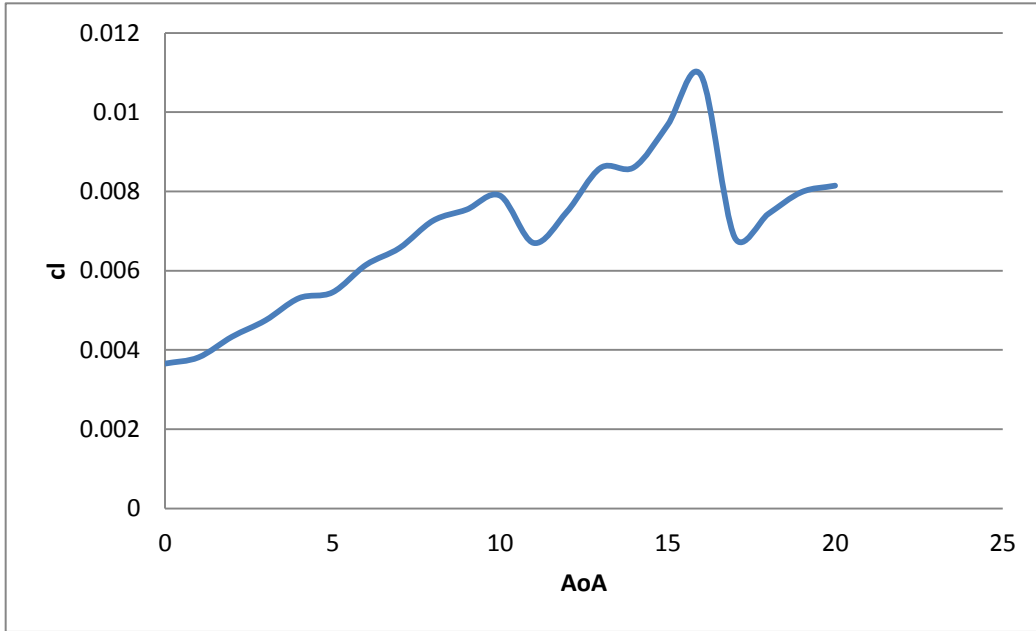


Figure 4.21: coefficient of lift vs AOA at 55 m/s

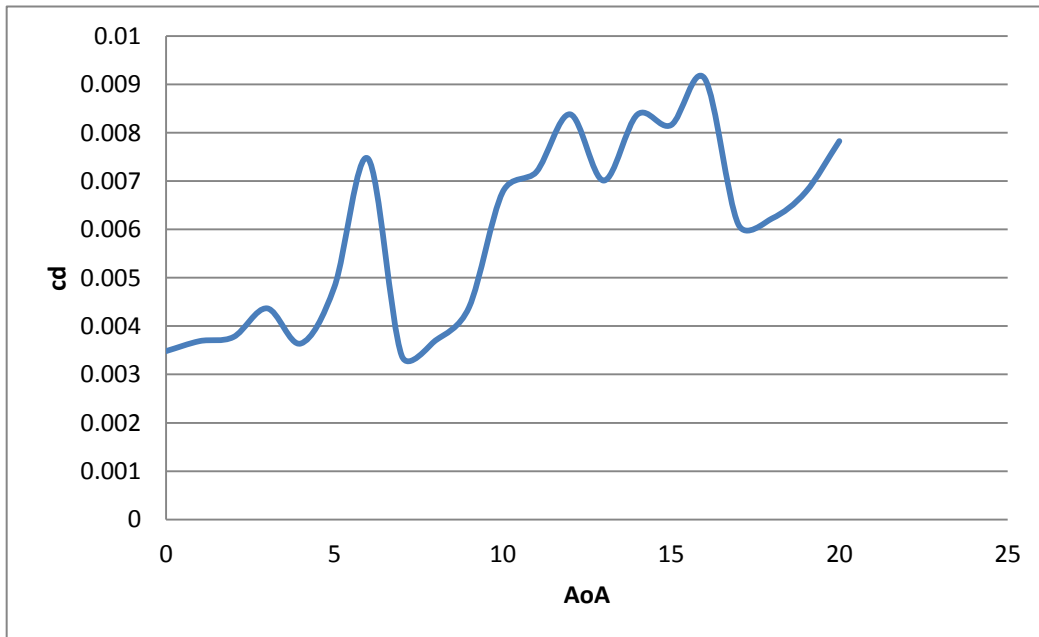


Figure 4.22: coefficient of drag vs AOA at 55 m/s

Angle of Attack (degree)	Lift force	Coefficient of lift	Drag force	Coefficient of drag
0	7.19	0.003379	6.64	0.003121
1	8.16	0.003835	7.45	0.003502
2	10.26	0.004822	7.75	0.003643
3	10.57	0.004968	8.7	0.004089
4	10.98	0.005161	6.99	0.003285
5	12.7	0.005969	5.66	0.00266
6	13.55	0.006369	10.96	0.005151
7	14.11	0.006632	5.91	0.002778
8	15.15	0.007121	5.94	0.002792
9	16.91	0.007948	6	0.00282
10	17.61	0.008277	12.91	0.006068
11	18.33	0.008615	16.53	0.007769
12	18.75	0.008813	18.19	0.00855
13	19.53	0.009179	18.45	0.008672
14	20.87	0.009809	19.74	0.009278
15	21.21	0.009969	21.94	0.010312
16	21.75	0.010223	23.09	0.010853
17	15.28	0.007182	13.04	0.006129
18	16.59	0.007798	16.6	0.007802
19	17.34	0.00815	17.25	0.008108
20	19.37	0.009104	19.01	0.008935

Table 4.10: coefficient of lift & drag at 60 m/s

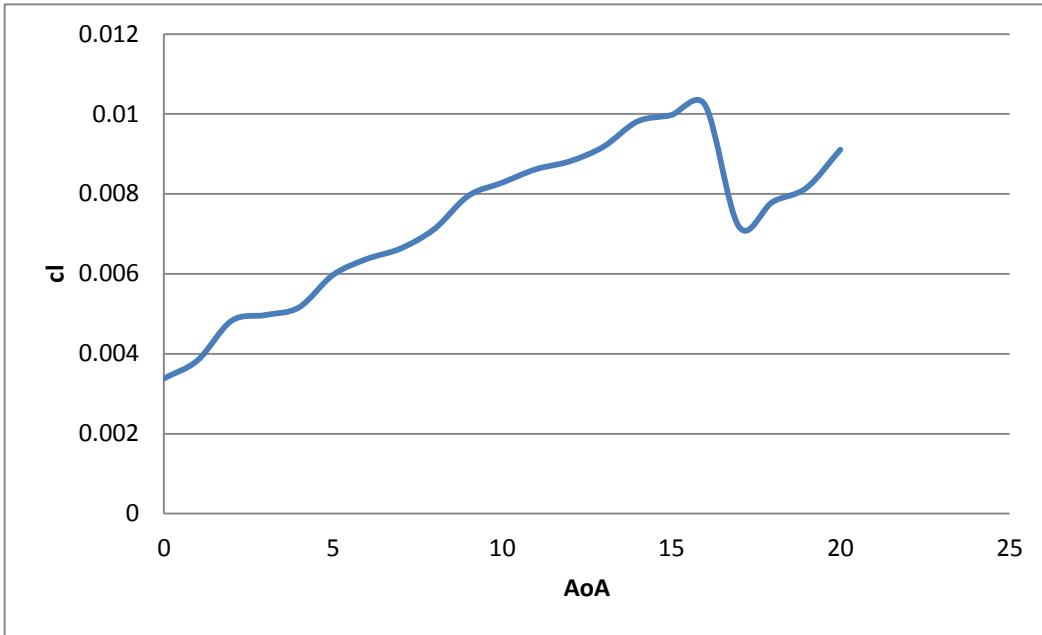


Figure 4.23: coefficient of lift vs AOA at 60 m/s

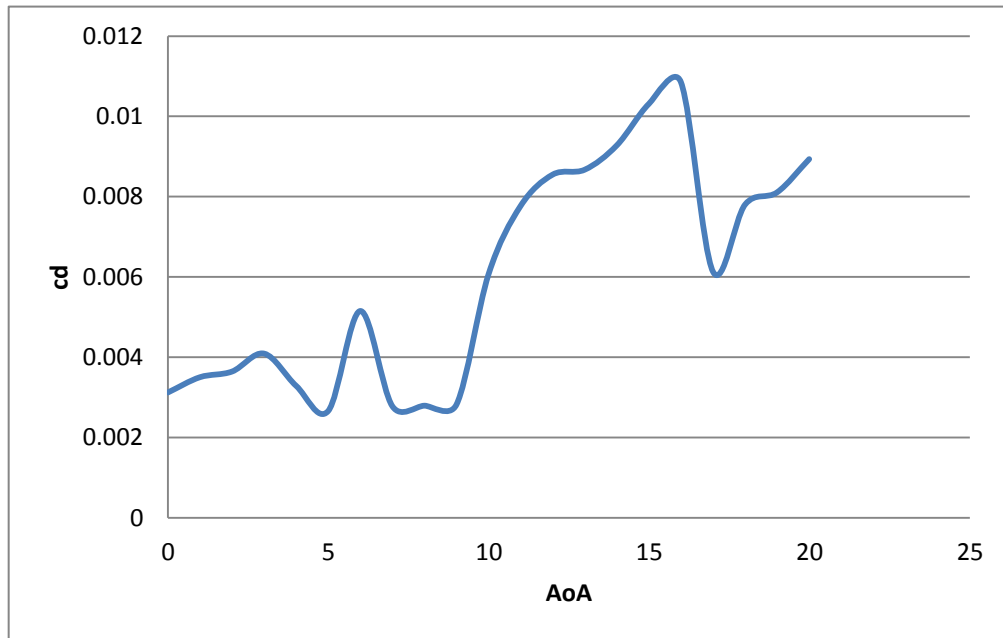
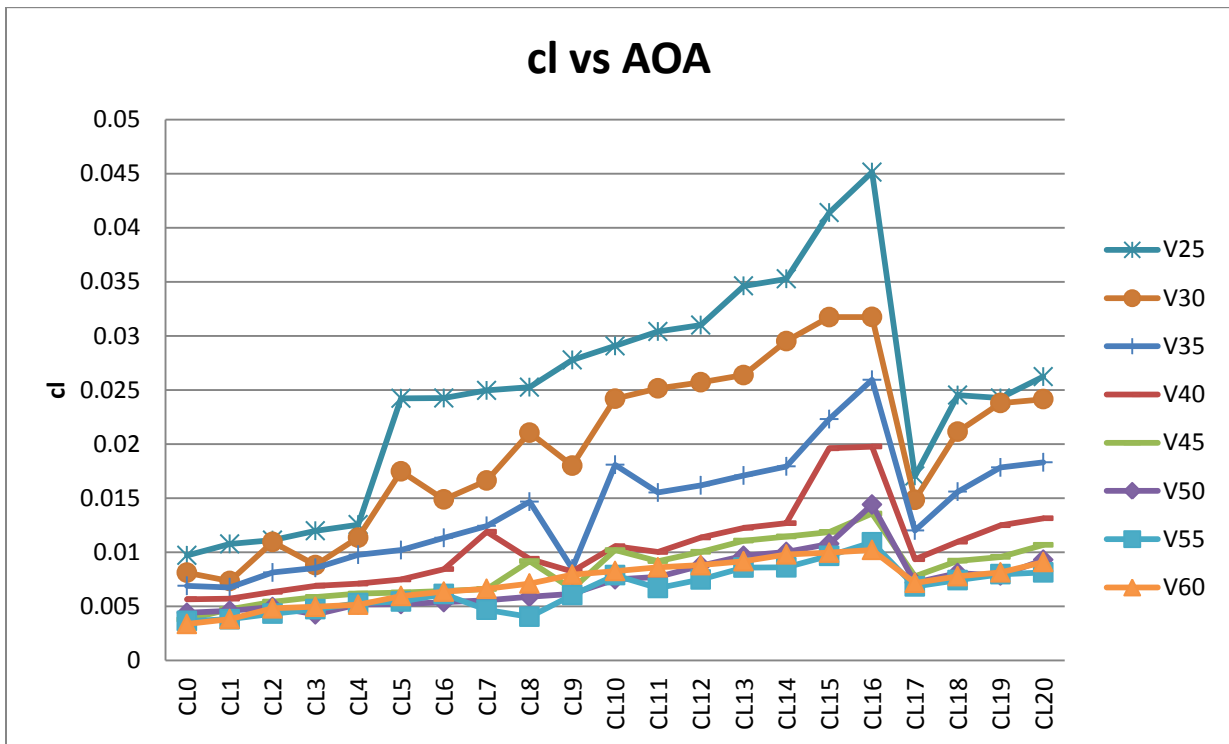
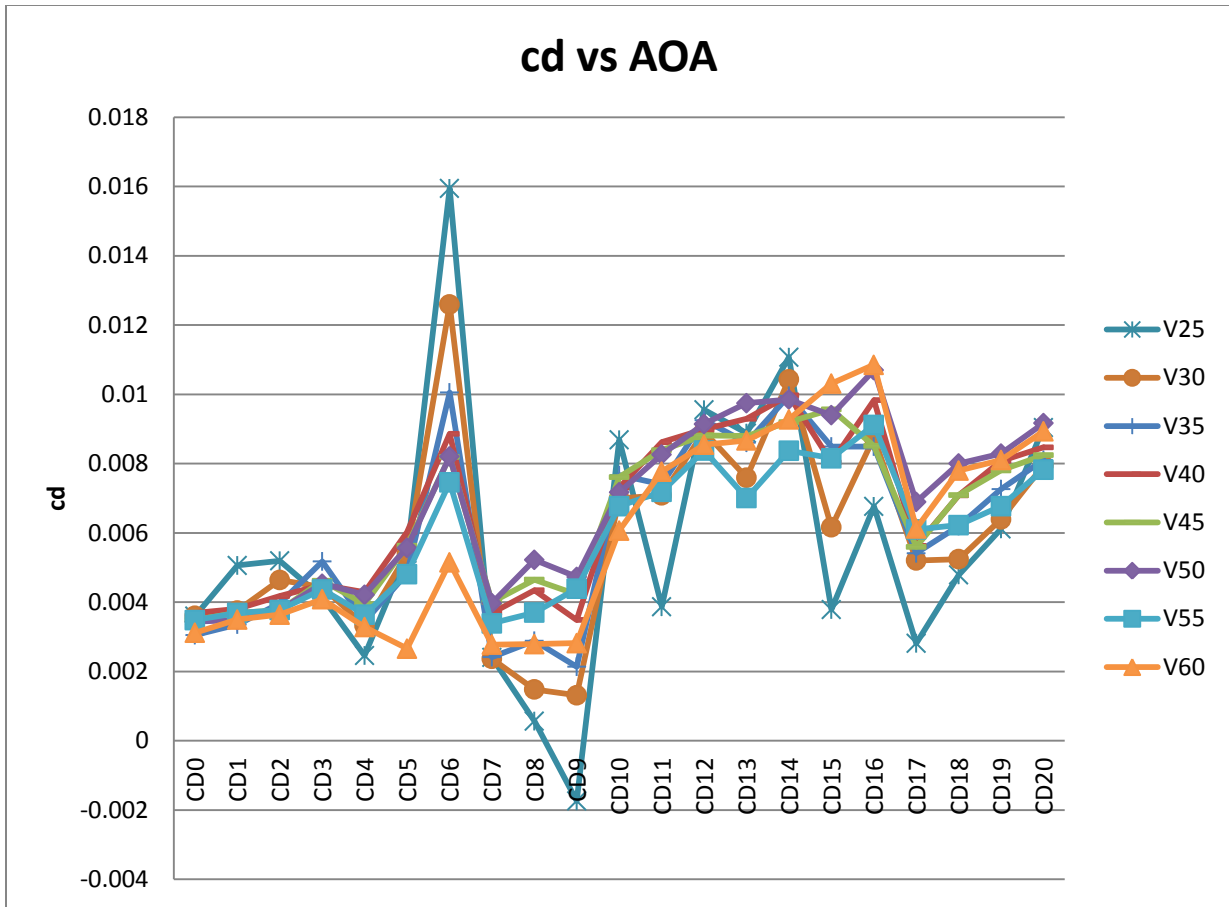


Figure 4.24: coefficient of drag vs AOA at 60 m/s



4.4.2 Analysis of experimental results on the characteristics of coefficient of lift and coefficient of drag.

Free stream velocity (m/s)	Coefficient of lift	Stall angle (degree)
25	0.017056	17
30	0.014852	17
35	0.012017	17
40	0.093596	17
45	0.007788	17
50	0.071950	17
55	0.068460	17
60	0.007182	17

Table 4.11: coefficient of lift at stall angle at various free stream velocity

4.4.3 Analysis of the coefficient of lift vs Angle of Attack

In the first experiment (at $v=25$ m/s) the lift increases when the angle of attack increases from 0° to 16° and decreases at the angle 17° . The coefficient of lift is 0.017056 at the stall angle 17° , as shown in figure 4.1. At the free stream velocity of 30 m/s the lift increases as the angle of attack increases from 0° to 16.5° and decreases at the angle 17° , as shown in figure 4.3 and the coefficient of lift is equal to 0.014852. Meanwhile the coefficient of lift increases from 0° to 16° and decreases at the angle 17° , at the free stream velocity of 35 m/s, 40 m/s, 45 m/s, 50 m/s, 55 m/s and 60 m/s as shown from figure 4.5 till 4.15.

The coefficient of lift are 0.012017, 0.093596, 0.007788, 0.071950, 0.068460, 0.007182 at the angle 17° for the free stream velocity of 35 m/s, 40 m/s, 45 m/s, 50 m/s, 55 m/s and 60 m/s respectively. The results shows that the coefficient of lift increases up to the stall angle which in this case ranges from 16.5° to 17° and decreases after the stall angle. The maximum lift that the MAV produced was at the angle 16° which was just before the stall angle. By comparing the lift force of at different free stream velocities, it will be found that the higher the speed the higher the force. The higher the angle the higher lift the MAV can achieve.

It can be seen from the graphs plotted previously that the lift at low angles of attack is oscillating, this is due to the instability of the wind tunnel reading. At low speed and low angles of attack the wind tunnel does not give accurate readings.

4.4.4 Analysis of the coefficient of drag vs Angle of Attack

From the experiments done on the wind tunnel the values of drag are not synchronized, this is due to the inaccuracy of the wind tunnel, the most common thing between drag graphs is that the highest drag at different free stream velocities is at the stall angle, which is 17° . Which shows that the higher the angle the higher the drag force, but still the results are not that accurate compared to the results obtained for the lift force, this is because the drag force is very sensitive and can be affected by the least disturbance. The graphs shows that turbulence in the air increases with higher velocities and higher angles of attack.

4.5.1 Experimental results on the characteristics of coefficient of lift, coefficient of drag and Reynolds number.

Velocity (m/s)	Coefficient of lift	Coefficient of drag	Reynolds number
25	0.009719	0.003601	1.44E+06
30	0.008122	0.00361	1.73E+06
35	0.006906	0.003053	2.02E+06
40	0.005668	0.003691	2.31E+06
45	0.003785	0.003484	2.60E+06
50	0.004406	0.003438	2.89E+06
55	0.003658	0.003485	3.18E+06
60	0.003379	0.003121	3.46E+06

Table 4.12: coefficient of lift & drag at 0° Angle of Attack

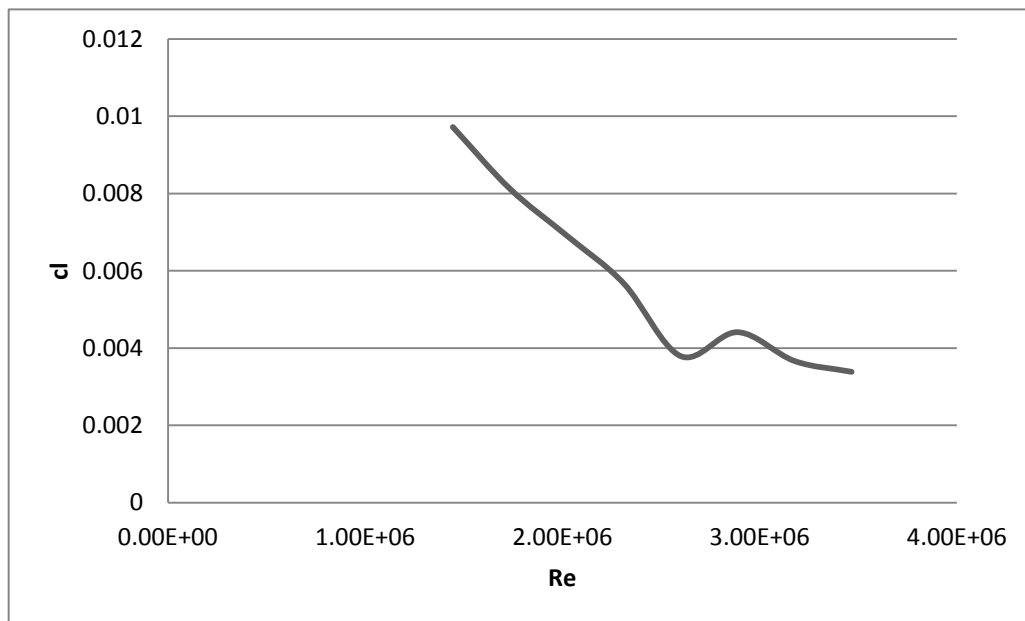


Figure 4.25: coefficient of lift vs Re at 0° AOA

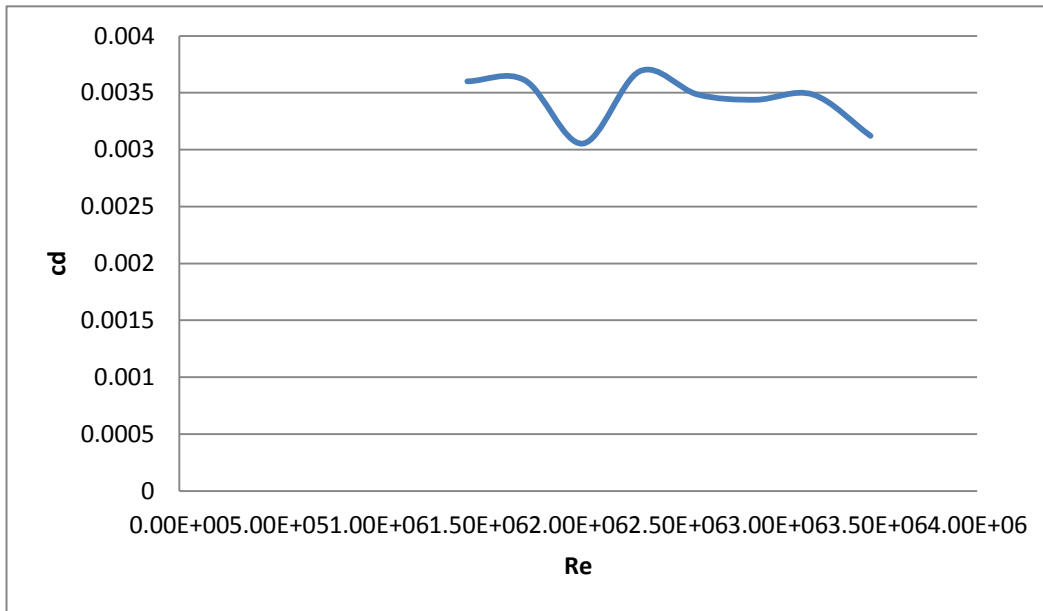


Figure 4.26: coefficient of drag vs Re at 0° AOA

Velocity (m/s)	Coefficient of lift	Coefficient of drag	Reynolds number
25	0.011127	0.005198	1.44E+06
30	0.010961	0.004644	1.73E+06
35	0.008136	0.003964	2.02E+06
40	0.006345	0.004177	2.31E+06
45	0.00544	0.00376	2.60E+06
50	0.004941	0.00377	2.89E+06
55	0.004335	0.003776	3.18E+06
60	0.004822	0.003643	3.46E+06

Table 4.13: coefficient of lift & drag at 2° Angle of Attack

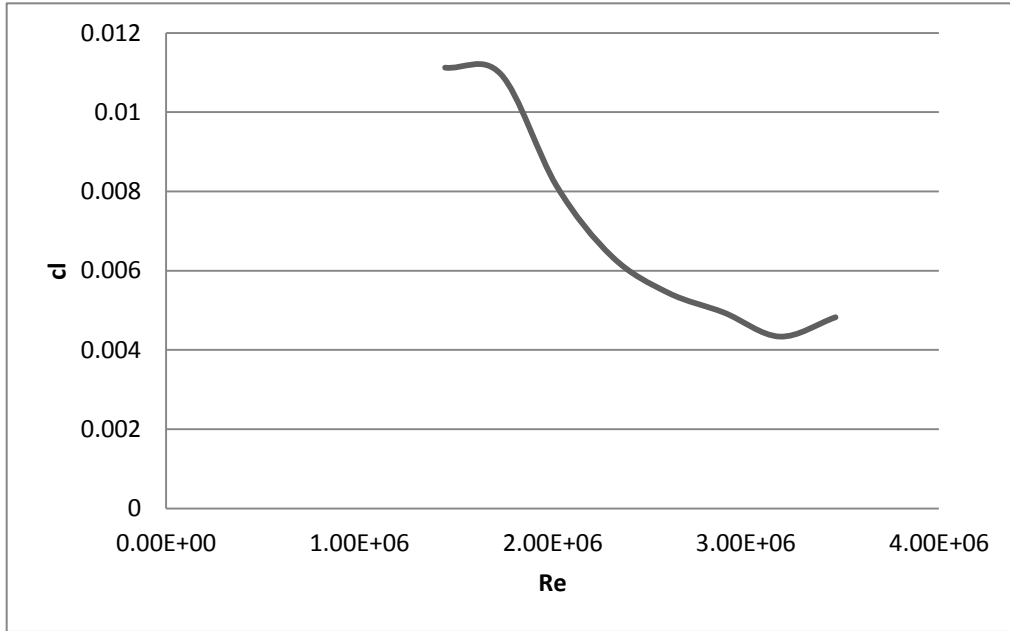


Figure 4.27: coefficient of lift vs Re at 2° AOA

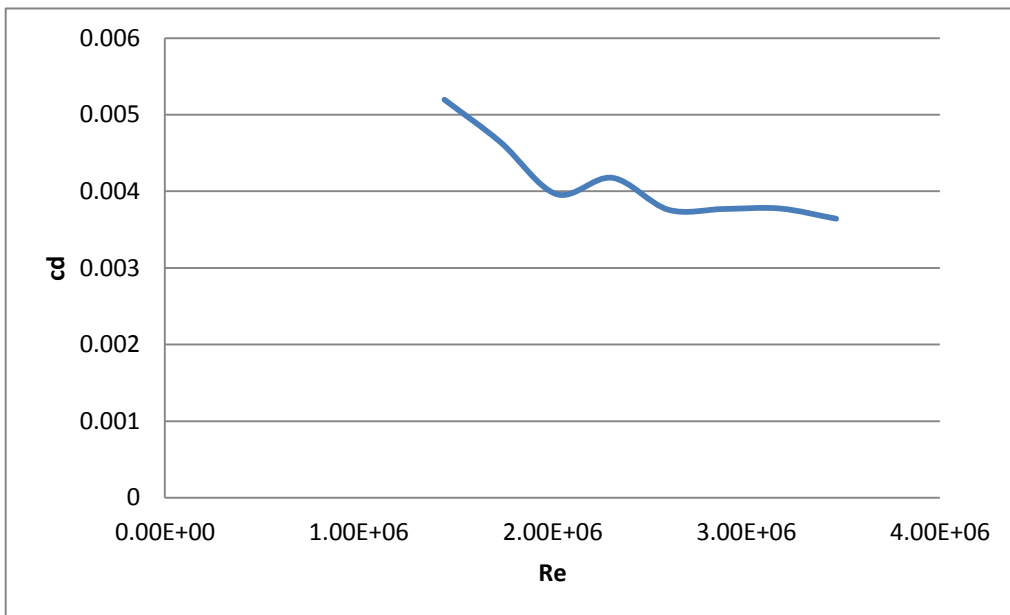


Figure 4.28: coefficient of drag vs Re at 2° AOA

Velocity (m/s)	Coefficient of lift	Coefficient of drag	Reynolds number
25	0.012562	0.002464	1.44E+06
30	0.011356	0.003328	1.73E+06
35	0.009779	0.003439	2.02E+06
40	0.007107	0.004294	2.31E+06
45	0.006183	0.003944	2.60E+06
50	0.005184	0.004217	2.89E+06
55	0.005308	0.003641	3.18E+06
60	0.005161	0.003285	3.46E+06

Table 4.14: coefficient of lift & drag at 4° Angle of Attack

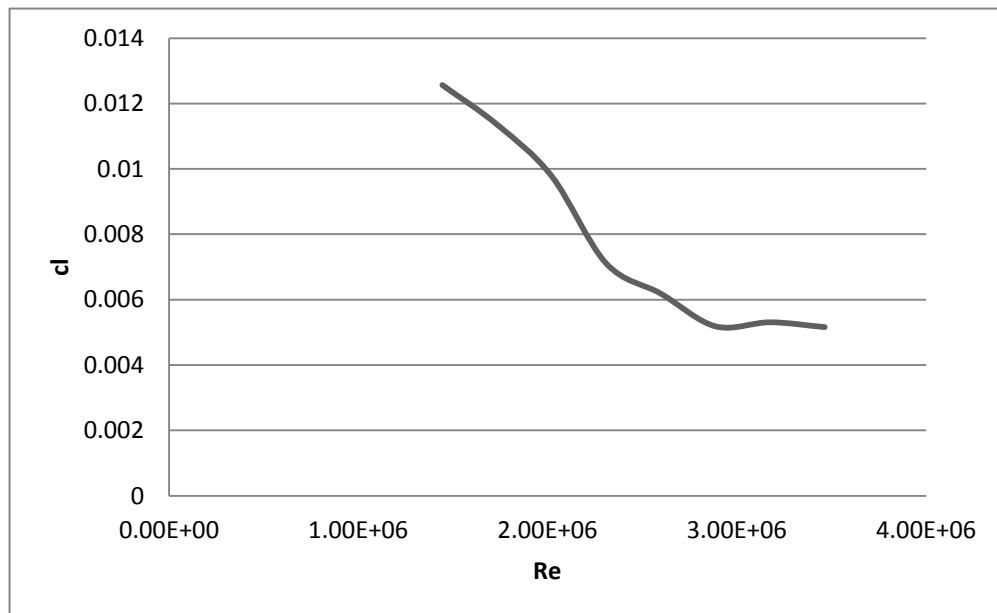


Figure 4.29: coefficient of lift vs Re at 4° AOA

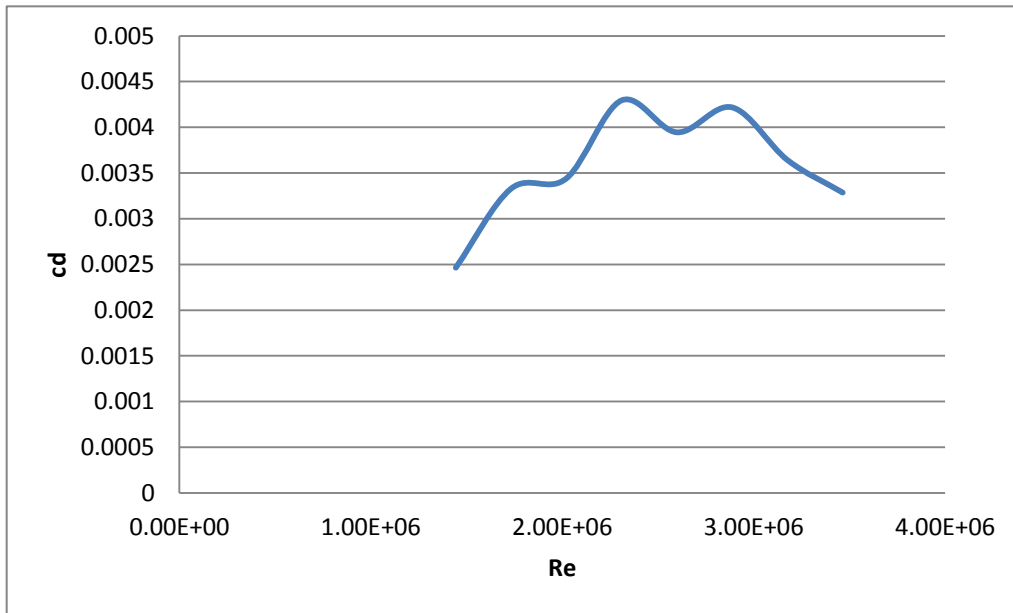


Figure 4.30: coefficient of drag vs Re at 4° AOA

Velocity (m/s)	Coefficient of lift	Coefficient of drag	Reynolds number
25	0.024257	0.015946	1.44E+06
30	0.017842	0.012596	1.73E+06
35	0.01134	0.010056	2.02E+06
40	0.00845	0.008862	2.31E+06
45	0.006434	0.008197	2.60E+06
50	0.005394	0.00821	2.89E+06
55	0.006147	0.007462	3.18E+06
60	0.006369	0.005151	3.46E+06

Table 4.15: coefficient of lift & drag at 6° Angle of Attack

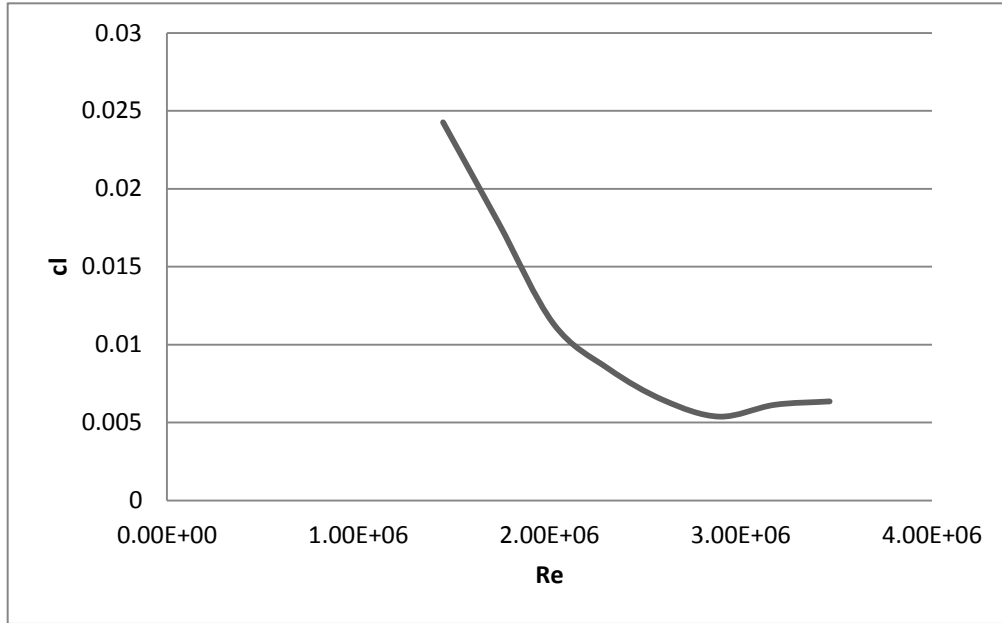


Figure 4.31: coefficient of lift vs Re at 6° AOA

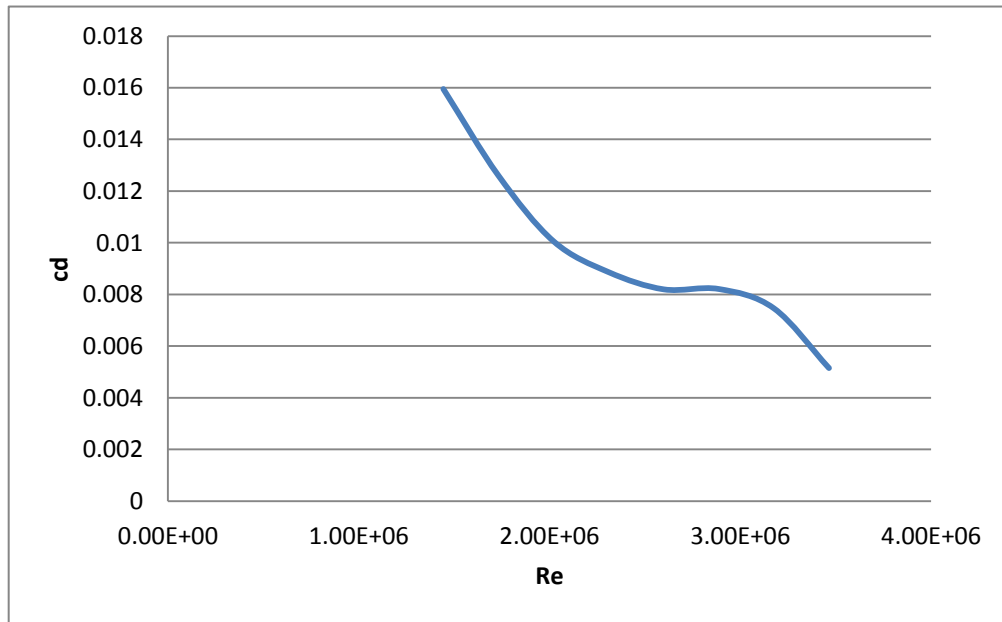


Figure 4.32: coefficient of drag vs Re at 6° AOA

Velocity (m/s)	Coefficient of lift	Coefficient of drag	Reynolds number
25	0.025259	0.000569	1.44E+06
30	0.022316	0.001485	1.73E+06
35	0.014683	0.002887	2.02E+06
40	0.009401	0.004346	2.31E+06
45	0.009183	0.004654	2.60E+06
50	0.005888	0.005225	2.89E+06
55	0.00726	0.003703	3.18E+06
60	0.007121	0.002792	3.46E+06

Table 4.16: coefficient of lift & drag at 8° Angle of Attack

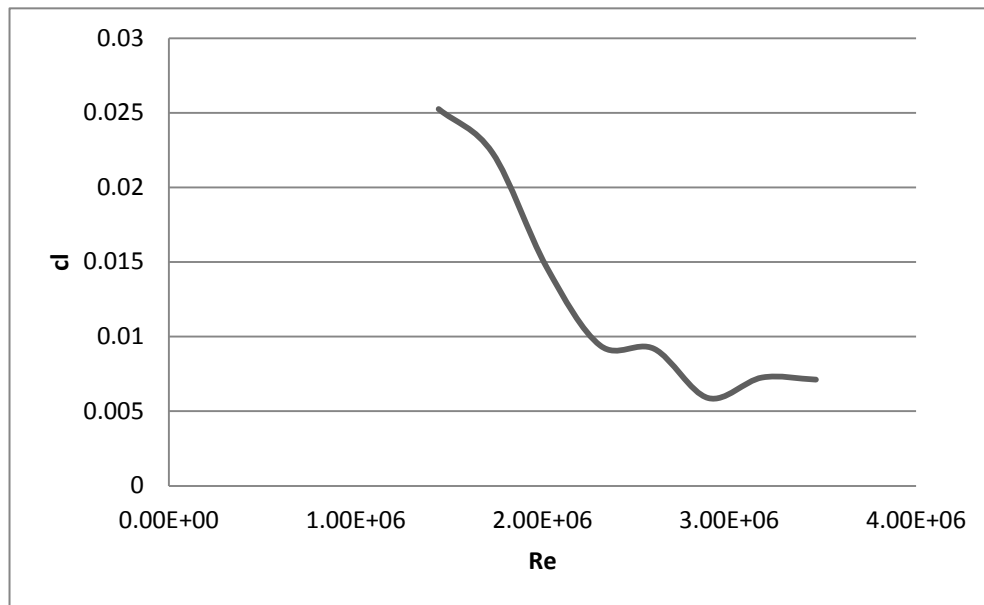


Figure 4.33: coefficient of lift vs Re at 8° AOA

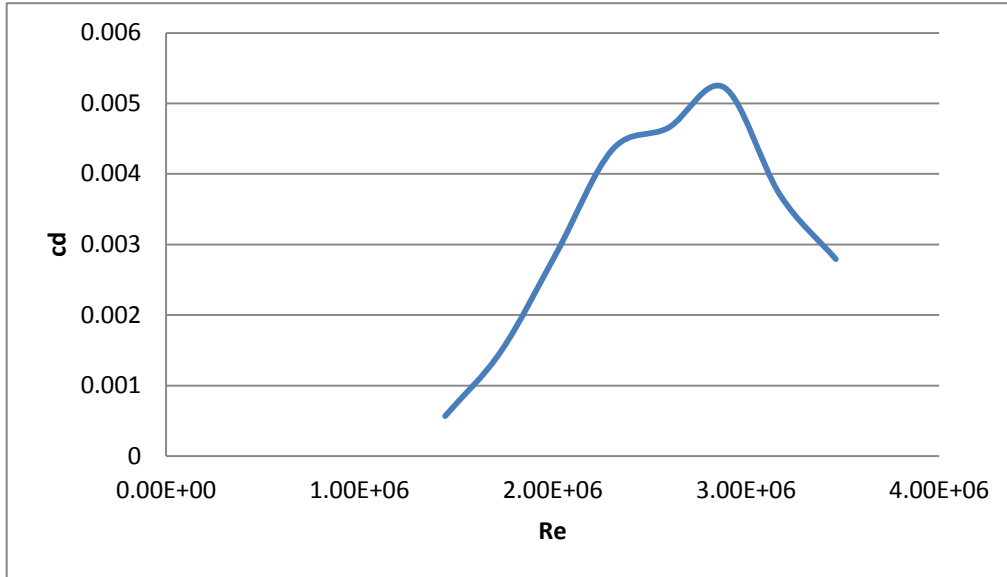


Figure 4.34: coefficient of drag vs Re at 8° AOA

Velocity (m/s)	Coefficient of lift	Coefficient of drag	Reynolds number
25	0.029076	0.00869	1.44E+06
30	0.024196	0.006994	1.73E+06
35	0.018095	0.007666	2.02E+06
40	0.010565	0.007308	2.31E+06
45	0.010202	0.007612	2.60E+06
50	0.007506	0.007174	2.89E+06
55	0.007892	0.006774	3.18E+06
60	0.008277	0.006068	3.46E+06

Table 4.17: coefficient of lift & drag at 10° Angle of Attack

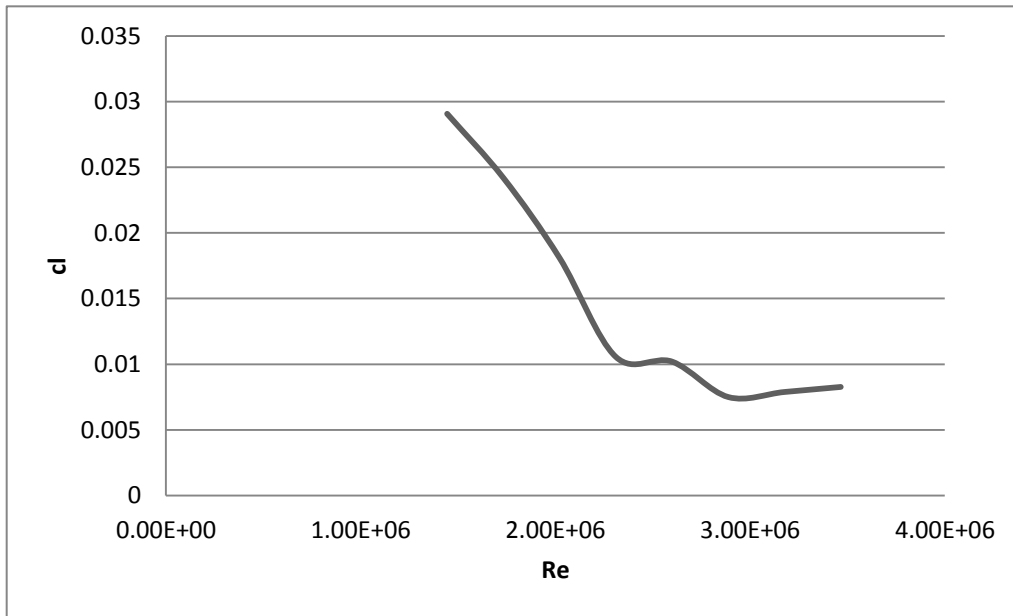


Figure 4.35: coefficient of lift vs Re at 10° AOA

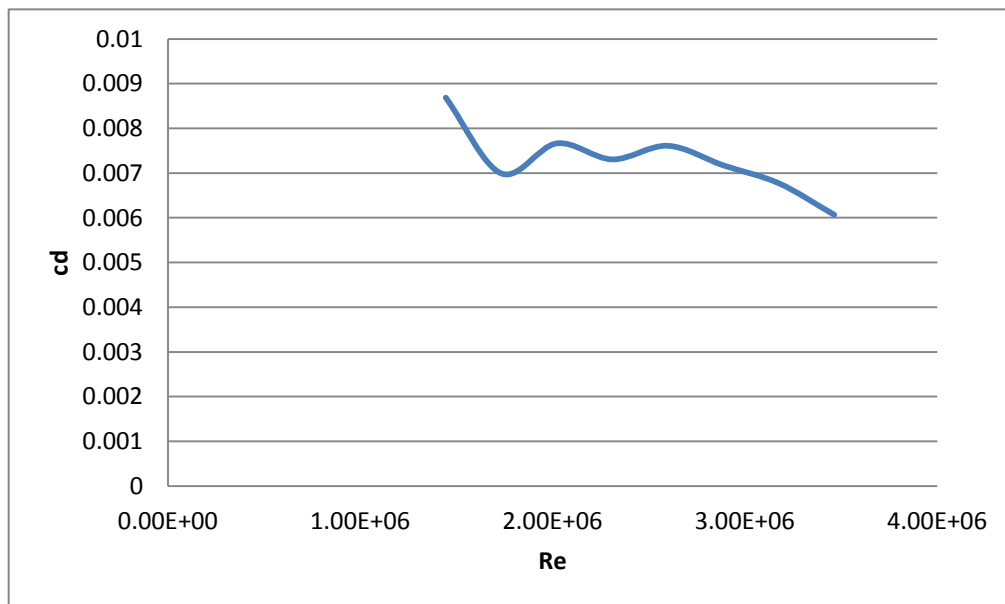


Figure 4.36: coefficient of drag vs Re at 10° AOA

Velocity (m/s)	Coefficient of lift	Coefficient of drag	Reynolds number
25	0.030998	0.009557	1.44E+06
30	0.025719	0.00893	1.73E+06
35	0.016188	0.009254	2.02E+06
40	0.011368	0.008989	2.31E+06
45	0.010044	0.008815	2.60E+06
50	0.008778	0.009144	2.89E+06
55	0.00749	0.008379	3.18E+06
60	0.008813	0.00855	3.46E+06

Table 4.18: coefficient of lift & drag at 12° Angle of Attack

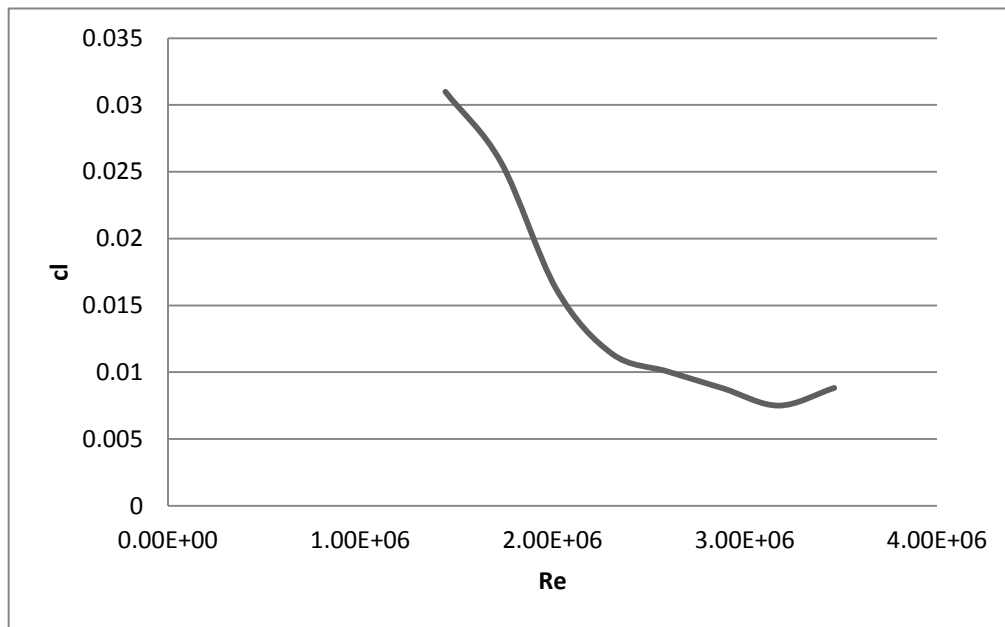


Figure 4.37: coefficient of lift vs Re at 12° AOA

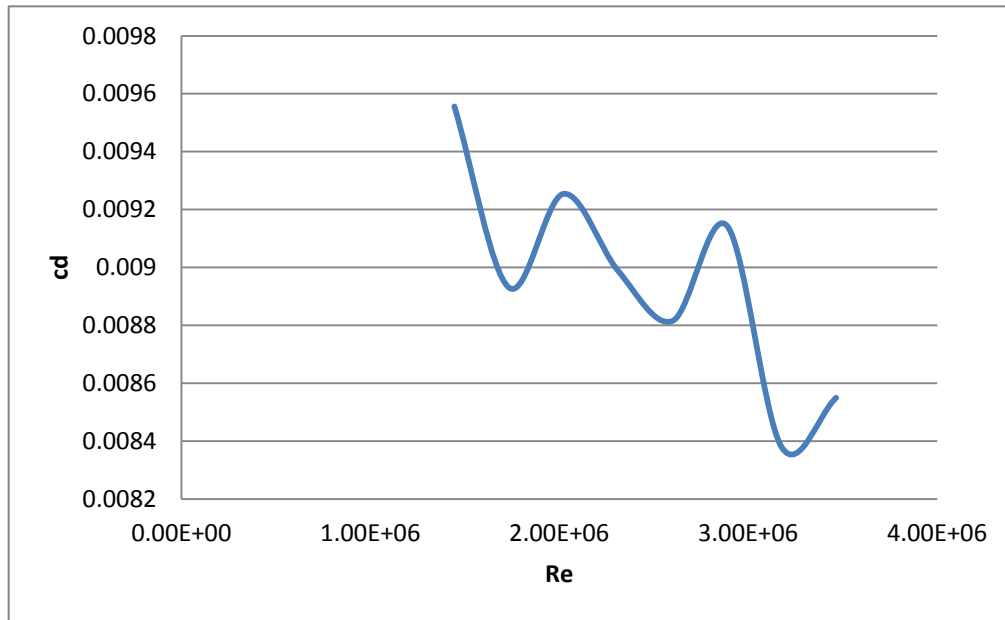


Figure 4.38: coefficient of drag vs Re at 12° AOA

Velocity (m/s)	Coefficient of lift	Coefficient of drag	Reynolds number
25	0.035276	0.011073	1.44E+06
30	0.029517	0.010434	1.73E+06
35	0.017943	0.009959	2.02E+06
40	0.01269	0.009973	2.31E+06
45	0.011464	0.0092	2.60E+06
50	0.01003	0.009854	2.89E+06
55	0.008608	0.008374	3.18E+06
60	0.009809	0.009278	3.46E+06

Table 4.19: coefficient of lift & drag at 14° Angle of Attack

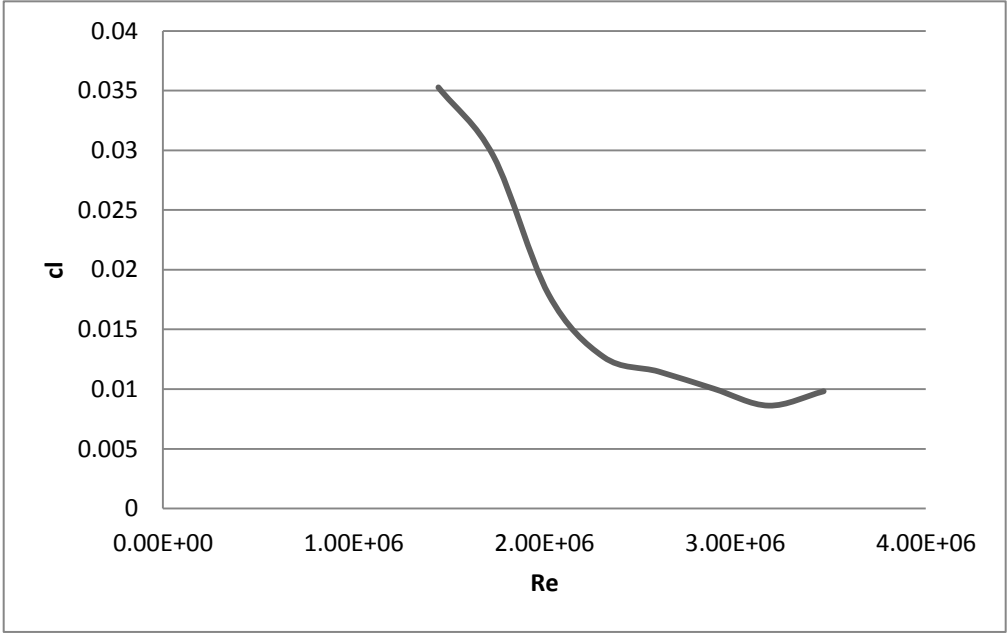


Figure 4.39: coefficient of lift vs Re at 14° AOA

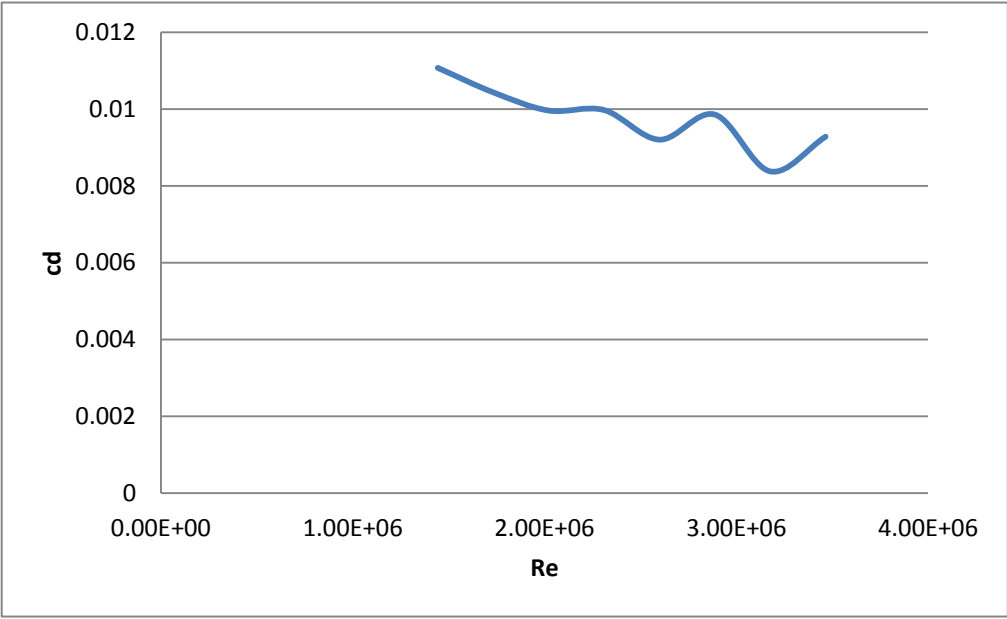


Figure 4.40: coefficient of drag vs Re at 14° AOA

Velocity (m/s)	Coefficient of lift	Coefficient of drag	Reynolds number
25	0.04513	0.006768	1.44E+06
30	0.031754	0.008761	1.73E+06
35	0.02594	0.008495	2.02E+06
40	0.019776	0.009835	2.31E+06
45	0.013578	0.008515	2.60E+06
50	0.014416	0.010701	2.89E+06
55	0.010924	0.009117	3.18E+06
60	0.010223	0.010853	3.46E+06

Table 4.20: coefficient of lift & drag at 16° Angle of Attack

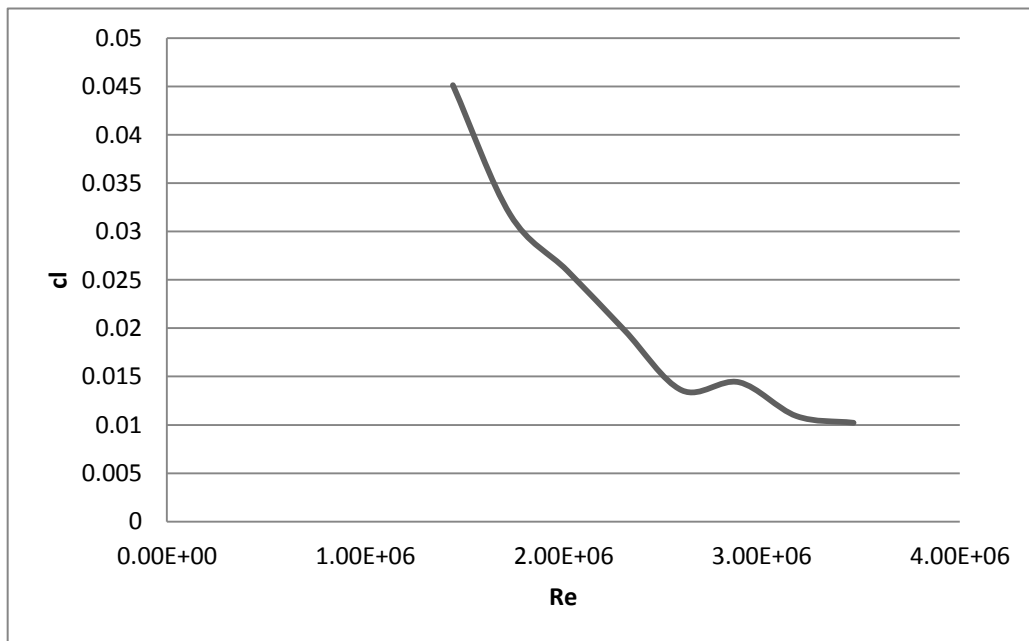


Figure 4.41: coefficient of lift vs Re at 16° AOA

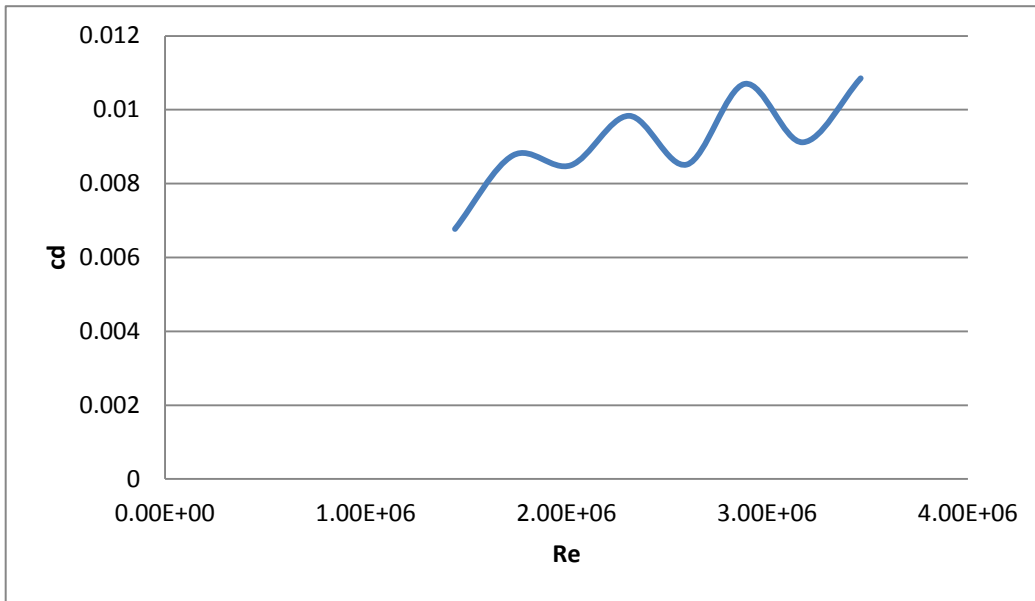


Figure 4.42: coefficient of drag vs Re at 16° AOA

Velocity (m/s)	Coefficient of lift	Coefficient of drag	Reynolds number
25	0.024528	0.004792	1.44E+06
30	0.021151	0.005245	1.73E+06
35	0.015608	0.006202	2.02E+06
40	0.010977	0.007085	2.31E+06
45	0.009225	0.007094	2.60E+06
50	0.008081	0.008007	2.89E+06
55	0.007428	0.006226	3.18E+06
60	0.007798	0.007802	3.46E+06

Table 4.21: coefficient of lift & drag at 18° Angle of Attack

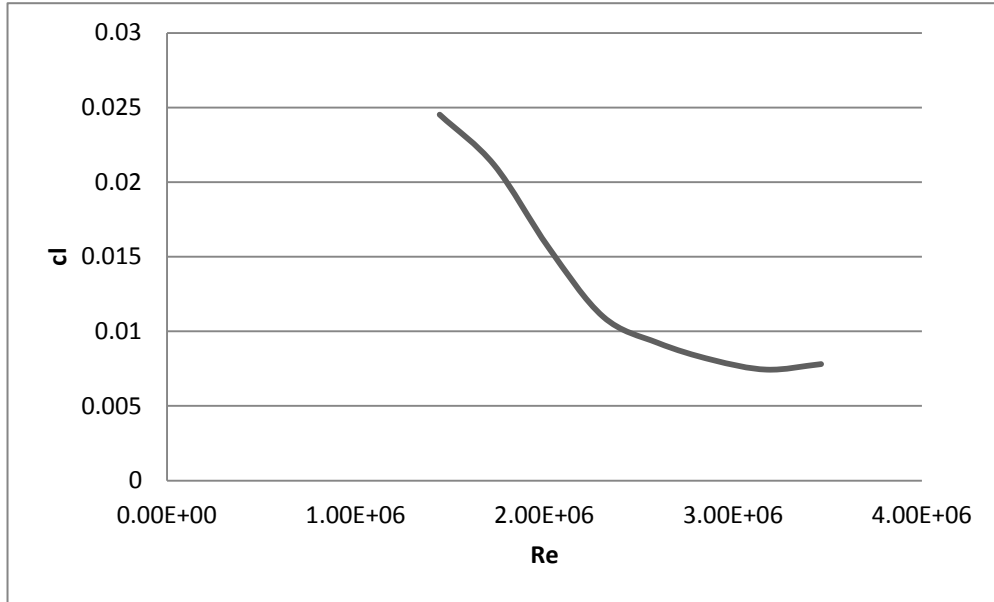


Figure 4.43: coefficient of lift vs Re at 18° AOA

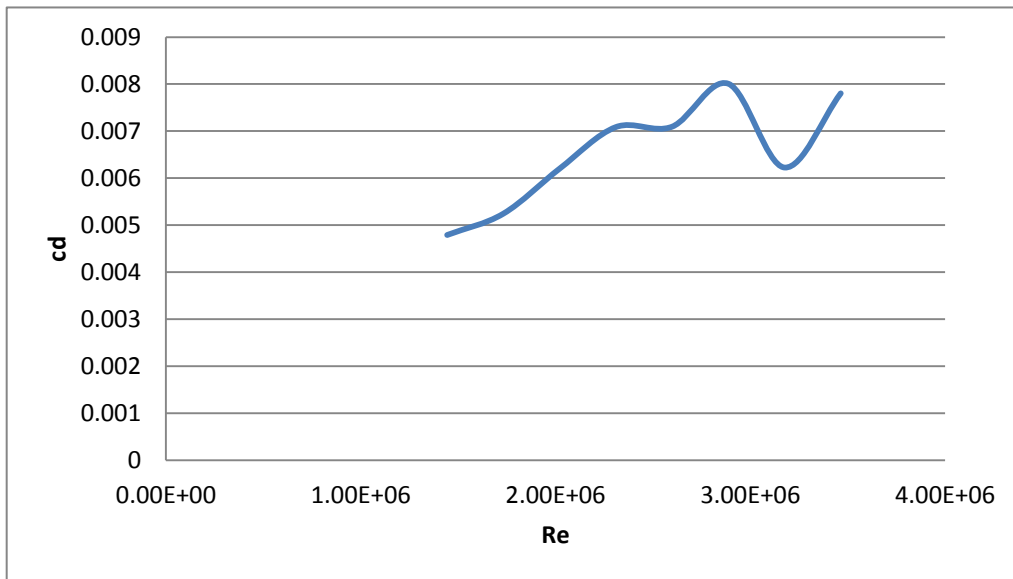


Figure 4.44: coefficient of drag vs Re at 18° AOA

Velocity (m/s)	Coefficient of lift	Coefficient of drag	Reynolds number
25	0.026234	0.009042	1.44E+06
30	0.024159	0.007953	1.73E+06
35	0.018316	0.008108	2.02E+06
40	0.013145	0.008471	2.31E+06
45	0.010687	0.008247	2.60E+06
50	0.009313	0.009171	2.89E+06
55	0.008144	0.007825	3.18E+06
60	0.009104	0.008935	3.46E+06

Table 4.22: coefficient of lift & drag at 20° Angle of Attack

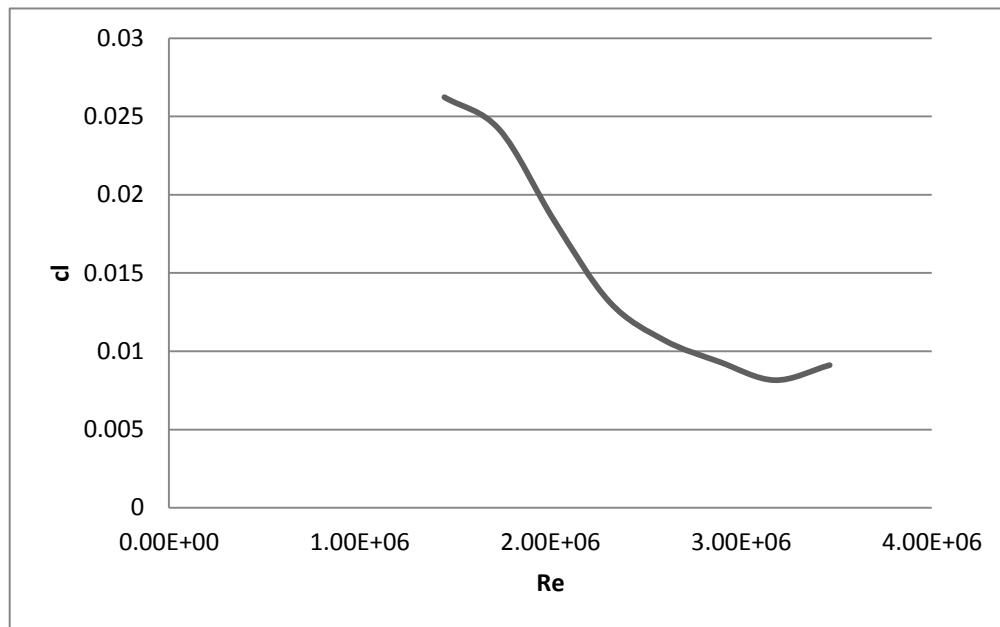


Figure 4.45: coefficient of lift vs Re at 20° AOA

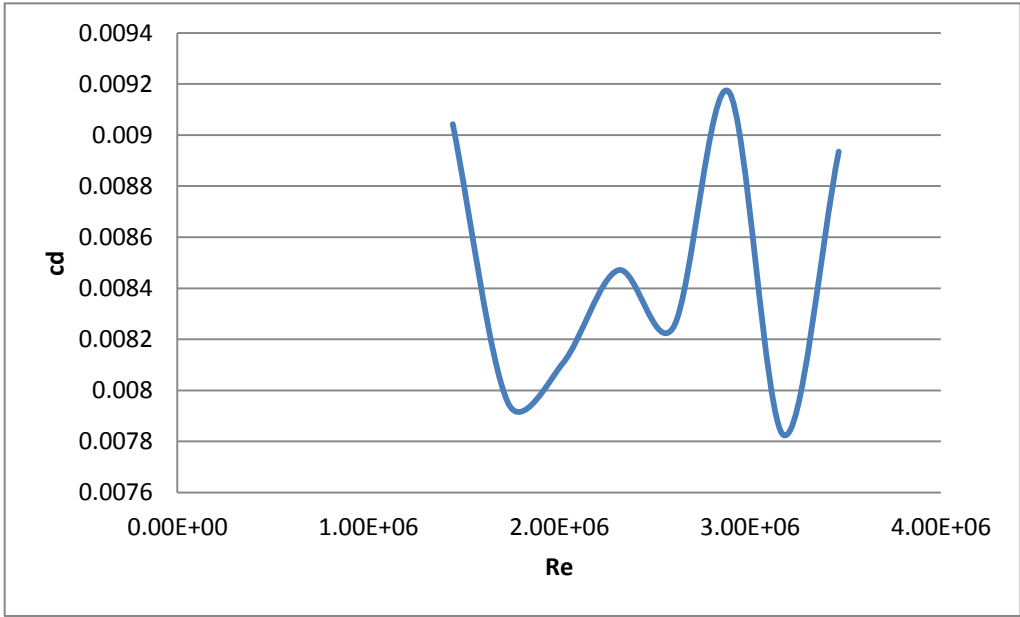


Figure 4.46: coefficient of drag vs Re at 20° AOA

4.5.2 Analysis of the coefficient of lift and drag vs Reynolds number

As shown in the tables and the graphs, it can be seen that by comparing the result of different angles of attack, when the angle increase the lift coefficient increase, but when the Reynolds number increase the lift coefficient decrease, which can be seen from the graphs plotted previously. As for the drag force, by increasing the angle of attack and the velocity the drag starts to increase, but at the same time at some speed the drag decreases, this is due to the instability of the readings.

So as a conclusion from these graphs as long as the velocity increases the lift force will increase, but at the same time the drag force will increase, which decreases the aerodynamics efficiency.

The aerodynamics efficiency is the to operate the MAV at its maximum L/D operating point, which actually is the problem statement of designing the MAV, so the main challenge here is to try increasing the efficiency, and by that the lift has to increase more and the drag decrease, so the maximum operating point can be achieved.

With the increase of Reynolds number the lift coefficient decreases and the drag coefficient increases, this is due to the Reynolds number equations, which shows that, with the increase of the velocity the Reynolds number increases, and the equation of the coefficient of lift shows that with the increase of the velocity the coefficient of lift decreases, which shows that the lift coefficient is inversely proportional with the Reynolds number.

Drag force increase with the increase of the angle of attack and Reynolds number, this is due to the increase of the air resistance to the object passing through the fluid, and by increasing the angle of attack, there is a bigger area facing the fluid, which contributes in more air resistance which leads to a higher drag, so the increase of Reynolds number will cause in the increasing of the AOA and Re.

CHAPTER 5

CONCLUSION AND RECOMMENDATION

5.1 CONCLUSION:

The experimental study on the effects of turbulence on a MAV model has reflected good design analysis regarding to, it's a preliminary design, which is a good step in developing a MAV. The experimental results show that the lift and drag increases with the increase the velocity and the angle of attack. The design has to be improved to enhance the lift required to overcome the drag at low velocities and low angles of attack.

The aerodynamic efficiency has to increase in order to enhance the aerodynamics characteristics, and by that the lift has to increase over the drag, because as high as the ratio of lift to drag increase as high the efficiency will be.

Lift force is not high enough, so the aerofoil of the MAV has to be larger, the problem of increasing the aerofoil, the area of the MAV will increase and by that the drag force will also increase, so another way has to found in order to achieve higher lift with lower drag MAV.

5.2 RECOMMENDATION:

The design should improved using CFD programs, in order to come up with a better design, the average of a MAV lift result is 1, but for the AMSA the maximum lift the MAV achieved was 0.1, which is a good result for a first design, improvement has to be done, after developing another design, experimental work has to be done in order to get more accurate results. So a new aerofoil has to be attached to the MAV in order to increase the lift force and at the same time the drag has to be decreased.

REFERENCES

1. http://encarta.msn.com/encyclopedia_701610394/Unmanned_Aerial_Vehicle.html
2. Peter J. Kunz aerodynamics and design for ultra-low Reynolds number flight
3. <http://www.sciencecentral.com/category/5894733>
4. <http://www.richardseaman.com/Aircraft/AirShows/Nellis2005/Highlights/Predator1oClock.jpg>
5. <http://www.globalsecurity.org/military/library/budget/fy2001/dote/airforce/01globalhawk.html>
6. http://www.airforce-technology.com/projects/hunter/images/Hunter_1.jpg
7. <http://newsinfo.colostate.edu/news/874701246/images/CSU%20UAV%20Maiden%2013.JPG>
8. <http://aviationfans.com/images/4forces.jpg>
9. Pedro J. Boschetti, Elsa M. Cárdenas, Andrea Amerio; Aerodynamic Optimization of an UAV Design
10. www.wikipedia.com
11. Antonio F.; flight performance of fixed and rotary wing aircraft; butterworth-heinmann 2006.
12. Clayton T, Donald F, John A; engineering fluid mechanics; wiley international edition. 8th edition 2005

13. W. Shyy, Y. Lian, J. Tang, H. Liu, P. Trizila, B. Stanford, L. Bernal, C. Cesnik, P. Friedmann, P. Ifju. Computational Aerodynamics of Low Reynolds Number Plunging, Pitching and Flexible Wings for MAV Applications
14. Richard S. Shevell, fundamentals of flight, second edition
15. Henry E. Jones, Oliver D. Wong, Kevin W. Noonan, Deane G. Reis, Brendon D. Malovrh, U.S. Army Aero flight dynamics Directorate, AMRDEC, U. S. Army Research & Development Command, NASA Langley Research Center, Hampton, Virginia. Aerodynamics characteristics of two rotary wings UAV design.
16. Thomas J. Mueller, James C. Kellogg, Peter G. Ifju, Sergey V. Shkareyev, introduction of the design of fixed-wing Micro Aerial Vehicle.
17. Alain Pelletier and Thomas J. Mueller† University of Notre Dame, Notre Dame. Low Reynolds Number Aerodynamics of Low-Aspect-Ratio, Thin/Flat/Cambered-Plate Wings.
18. Matthew C. Shields, Cameron M. Hatcher, Roland A. Pitcairn, Christopher W. Aiken, David B. Berman, Christopher M. Carnahan, William A. Foley, Sean P. Hammervold, William E. Holway and Lindsay C. Marek University of Colorado, Boulder, Design and development of a reconnaissance Micro Aerial Vehicle.
19. Unmanned Aerial Vehicles for Rapid Environmental Assessment and Mine Counter measures, Manuel de Sousa, Maritime Operations Division, Defense Science and Technology Organization
20. Pedro J.B, Elsa M.C, Andrea A; aerodynamic optimization of an UAV design; AIAA American institute of aeronautics and astronautics.

21. Reverse Engineering and Aerodynamic Analysis of a Flying Wing UAV Navabalachandran s/o Jayabalan¹], Low Jun Horng², G. Leng³ Aeronautical Engineering Group Department of Mechanical Engineering National University of Singapore.
22. High altitude long endurance unmanned aerial vehicle of a new generation – a design challenge for a low cost, reliable and high performance aircraft, Z. GORAJ¹, A. FRYDRYCHEWICZ¹, R.ŚWITKIEWICZ¹, B.HERNIK¹, J. GADOMSKI¹,T. GOETZENDORF-GRABOWSKI¹, M. FIGAT¹, St. SUCHODOLSKI¹ and W. CHAJEC² Institute of Aeronautics and Applied Mechanics, Warsaw University of Technology.
23. Determination of the Aerodynamic Characteristics of Low Reynolds, Number Flows over Small Uninhabited Aerial Vehicles, Authors: Hugo T. C. Pedro, Dr. Marcelo H. Kobayashi (advisor)
24. Model Identification of a Micro Air Vehicle, Jorge Niño¹, Flavius Mitrasche¹, Peter Cosyn², Robin De Keyser¹, Department of Electrical Energy, Systems and Automation, Ghent University. Department of Flow, Heat and Combustion Mechanics, Ghent University
25. Multidisciplinary Design Optimization of Unmanned Aerial Vehicles (UAV) using Multi-Criteria Evolutionary Algorithms Luis. F. González¹, K. Srinivas¹, Jacques Périaux² and Eric J. Whitney¹, ¹School of Aerospace, Mechanical and Mechatronic Engineering, University of Sydney, Sydney, Australia.
26. THICKNESS EFFECT ON LOW-ASPECT-RATIO WING AERODYNAMIC CHARACTERISTICS AT A LOW REYNOLDS NUMBER F. B. Hsiao, C. Y. Lin , Y. C. Liu , D. B. Wang, Institute of Aeronautics and Astronautics National Cheng Kung University.

27. Multidisciplinary Design Optimization of UAV Airframes Andr_as S_obester_, Andy J. Keaney University of Southampton, Southampton, Hampshire.
28. Aerodynamic calculation of unmanned aircraft Marcin Figat, Tomasz Goetzendorf-Grabowski and Zdobysław Goraj Warsaw University of Technology, Warsaw, Poland.
29. Aerodynamic design assessment of Strato 2C and its potential for unmanned high altitude airborne platforms, Dirk Schawe *, Claas-Hinrik Rohardt, Georg Wichmann DLR – German Aerospace Center, Institute of Aerodynamics and Flow Technology, Lilienthalplatz.

APPENDIX I

Lift and Drag forces vs AOA at different velocities measured by the wind tunnel:

AOA	Lift force	Lift coefficient	Drag force	Drag coefficient
0	1.61	0.108968	0.06	0.004061
1	0.42	0.028426	0.08	0.005415
2	1.61	0.108968	0.1	0.006768
3	0.78	0.052792	0.23	0.015567
4	1.41	0.095431	0.15	0.010152
5	1.15	0.077834	0.28	0.018951
6	3.6	0.243655	4.53	0.306599
7	0.52	0.035195	0.17	0.011506
8	1.51	0.1022	-2.66	-0.18003
9	5.26	0.356007	-2.43	-0.16447
10	1.77	0.119797	0.11	0.007445
11	3.12	0.211168	-0.85	-0.05753
12	1.93	0.130626	-0.42	-0.02843
13	1.67	0.113029	-0.42	-0.02843
14	2.23	0.150931	-0.41	-0.02775
15	5.73	0.387817	-1.64	-0.111
16	6.61	0.447377	-1.25	-0.0846
17	1.2	0.081218	-0.17	-0.01151
18	5.78	0.391201	-1	-0.06768
19	5.57	0.376988	-1.06	-0.07174
20	5.88	0.39797	-0.74	-0.05008

Coefficient and force of lift & drag at 5 m/s

AOA	Lift force	Lift Coefficient	Drag force	Drag coefficient
0	0.47	0.007953	0.87	0.014721
1	1.87	0.031641	0.21	0.003553
2	1.82	0.030795	0.23	0.003892
3	2.39	0.04044	0.25	0.00423
4	3.59	0.060745	0.21	0.003553
5	2.9	0.049069	0.58	0.009814
6	4.48	0.075804	4.58	0.077496
7	2.14	0.03621	0.19	0.003215
8	2.97	0.050254	-2.3	-0.03892
9	6.78	0.114721	-2.15	-0.03638
10	3.33	0.056345	0.32	0.005415
11	4.74	0.080203	-0.21	-0.00355
12	3.7	0.062606	0.19	0.003215
13	3.33	0.056345	-0.08	-0.00135
14	3.84	0.064975	-0.1	-0.00169
15	7.45	0.126058	-1.08	-0.01827
16	8.8	0.1489	-1	-0.01692
17	3.85	0.065144	-0.08	-0.00135
18	7.86	0.132995	-0.6	-0.01015
19	7.4	0.125212	-0.74	-0.01252
20	7.67	0.12978	-0.13	-0.0022

Coefficient and force of lift & drag at 10 m/s

AOA	Lift force	Lift Coefficient	Drag force	Drag coefficient
0	2.4	0.018049	0.74	0.005565
1	2.52	0.018951	0.66	0.004963
2	2.19	0.016469	0.66	0.004963
3	2.97	0.022335	0.34	0.002557
4	3.5	0.026321	0.5	0.00376
5	4.7	0.035345	0.79	0.005941
6	5.5	0.041361	4.85	0.036473
7	6.12	0.046024	0.36	0.002707
8	5.1	0.038353	-2	-0.01504
9	9.38	0.07054	-1.72	-0.01293
10	4.22	0.031735	0.77	0.005791
11	5.62	0.042264	0.28	0.002106
12	6.3	0.047377	0.57	0.004287
13	6.47	0.048656	0.58	0.004362
14	6.88	0.051739	0.45	0.003384
15	9.95	0.074826	-0.4	-0.00301
16	11.56	0.086934	-0.4	-0.00301
17	6.61	0.049709	0.31	0.002331
18	10.16	0.076405	0.1	0.000752
19	10.29	0.077383	-0.32	-0.00241
20	10.34	0.077759	0.15	0.001128

Coefficient and force of lift & drag at 15 m/s

AOA	Lift force	Lift Coefficient	Drag force	Drag coefficient
0	2.2	0.009306	1	0.00423
1	2.9	0.012267	1.11	0.004695
2	5.31	0.022462	1.19	0.005034
3	3.33	0.014086	1.29	0.005457
4	4.27	0.018063	0.89	0.003765
5	7.24	0.030626	1.52	0.00643
6	7.5	0.031726	5.49	0.023223
7	7.9	0.033418	0.77	0.003257
8	8.23	0.034814	-1.36	-0.00575
9	8.67	0.036675	-1.3	-0.0055
10	8.93	0.037775	1.57	0.006641
11	9.21	0.038959	1.13	0.00478
12	9.48	0.040102	1.26	0.00533
13	8.65	0.036591	1.28	0.005415
14	8.77	0.037098	2.01	0.008503
15	13.12	0.055499	-0.3	-0.00127
16	15.1	0.063875	1.2	0.005076
17	7.34	0.031049	0.5	0.002115
18	11.04	0.046701	0.68	0.002876
19	9.11	0.038536	0.58	0.002453
20	9.67	0.040905	1.2	0.005076

Coefficient and force of lift & drag at 20m/s

APPENDIX II

Lift and Drag forces vs reynolds number at differents AOA measured by the wind tunnel:

Velocity	Re	Lift force	Lift coefficient	Drag force	Drag coefficient
5	2.89E+04	0.42	0.028426	0.08	0.005415
10	5.77E+04	1.87	0.031641	0.21	0.003553
15	8.66E+04	2.52	0.018951	0.66	0.004963
20	1.15E+05	2.9	0.012267	1.11	0.004695

Coefficient and force of lift & drag vs reynolds number at 1° Angle of Attack

Velocity	Re	Lift force	Lift coefficient	Drag force	Drag coefficient
5	2.89E+04	0.78	0.052792	0.23	0.015567
10	5.77E+04	2.39	0.04044	0.25	0.00423
15	8.66E+04	2.97	0.022335	0.34	0.002557
20	1.15E+05	3.33	0.014086	1.29	0.005457

Coefficient and force of lift & drag vs reynolds number at 3° Angle of Attack

Velocity	Re	Lift force	Lift coefficient	Drag force	Drag coefficient
5	2.89E+04	1.15	0.077834	0.28	0.018951
10	5.77E+04	2.9	0.049069	0.58	0.009814
15	8.66E+04	4.7	0.035345	0.79	0.005941
20	1.15E+05	7.24	0.030626	1.52	0.00643

Coefficient and force of lift & drag vs reynolds number at 5° Angle of Attack

Velocity	Re	Lift force	Lift coefficient	Drag force	Drag coefficient
5	2.89E+04	0.52	0.035195	0.17	0.011506
10	5.77E+04	2.14	0.03621	0.19	0.003215
15	8.66E+04	6.12	0.046024	0.36	0.002707
20	1.15E+05	7.9	0.033418	0.77	0.003257

Coefficient and force of lift & drag vs reynolds numberat 7° Angle of Attack

Velocity	Re	Lift force	Lift coefficient	Drag force	Drag coefficient
5	2.89E+04	5.26	0.356007	-2.43	-0.16447
10	5.77E+04	6.78	0.114721	-2.15	-0.03638
15	8.66E+04	9.38	0.07054	-1.72	-0.01293
20	1.15E+05	8.67	0.036675	-1.3	-0.0055

Coefficient and force of lift & drag vs reynolds numberat 9° Angle of Attack

Velocity	Re	Lift force	Lift coefficient	Drag force	Drag coefficient
5	2.89E+04	3.12	0.211168	-0.85	-0.05753
10	5.77E+04	4.74	0.080203	-0.21	-0.00355
15	8.66E+04	5.62	0.042264	0.28	0.002106
20	1.15E+05	9.21	0.038959	1.13	0.00478

Coefficient and force of lift & drag vs reynolds numberat 11° Angle of Attack

Velocity	Re	Lift force	Lift coefficient	Drag force	Drag coefficient
5	2.89E+04	1.67	0.113029	-0.42	-0.02843
10	5.77E+04	3.33	0.056345	-0.08	-0.00135
15	8.66E+04	6.47	0.048656	0.58	0.004362
20	1.15E+05	8.65	0.036591	1.28	0.005415

Coefficient and force of lift & drag vs reynolds numberat 13° Angle of Attack

Velocity	Re	Lift force	Lift coefficient	Drag force	Drag coefficient
5	2.89E+04	5.73	0.387817	-1.64	-0.111
10	5.77E+04	7.45	0.126058	-1.08	-0.01827
15	8.66E+04	9.95	0.074826	-0.4	-0.00301
20	1.15E+05	13.12	0.055499	-0.3	-0.00127

Coefficient and force of lift & drag vs reynolds numberat 15° Angle of Attack

Velocity	Re	Lift force	Lift coefficient	Drag force	Drag coefficient
5	2.89E+04	1.2	0.081218	-0.17	-0.01151
10	5.77E+04	3.85	0.065144	-0.08	-0.00135
15	8.66E+04	6.61	0.049709	0.31	0.002331
20	1.15E+05	7.34	0.031049	0.5	0.002115

Coefficient and force of lift & drag vs reynolds numberat 17° Angle of Attack

Velocity	Re	Lift force	Lift coefficient	Drag force	Drag coefficient
5	2.89E+04	5.57	0.376988	-1.06	-0.07174
10	5.77E+04	7.4	0.125212	-0.74	-0.01252
15	8.66E+04	10.29	0.077383	-0.32	-0.00241
20	1.15E+05	9.11	0.038536	0.58	0.002453

Coefficient and force of lift & drag vs reynolds number at 19° Angle of Attack

APPENDIX III

Lift/drag coefficients vs the AOA and speed, which is the experimental result for the aerodynamic efficiency of the MAV

AOA	Lift/drag coefficient											
	Velocity											
	5m/s	10m/s	15m/s	20m/s	25m/s	30m/s	35m/s	40m/s	45m/s	50m/s	55m/s	60m/s
0	26.8	0.54	3.24	2.2	2.69	2.25	2.26	1.53	1.08	1.28	1.04	1.08
1	5.25	8.90	3.81	2.6	2.12	1.95	2.01	1.5	1.28	1.31	1.03	1.09
2	16.1	7.91	3.31	4.4	2.14	2.36	2.05	1.51	1.44	1.31	1.14	1.32
3	3.39	9.56	8.73	2.5	2.89	1.98	1.65	1.53	1.27	0.94	1.08	1.21
4	9.4	17.0	7	4.7	5.09	3.41	2.84	1.65	1.56	1.22	1.45	1.57
5	4.1	5	5.94	4.7	4.47	3.24	2.11	1.24	1.11	0.93	1.13	2.24
6	0.79	0.97	1.1	1.36	1.52	1.41	1.12	0.95	0.78	0.65	0.82	1.23
7	3.0	11.2	17	10.2	10.3	8.27	5.14	2.42	1.65	1.40	1.93	2.38
8	-0.56	-1.2	-2.55	-6.05	44.4	15	5.08	2.16	1.97	1.12	1.96	2.55
9	-2.1	-3.1	-5.4	-6.6	-16	17.7	8.24	2.90	2.31	1.30	1.71	2.81
10	16	10.4	5.48	5.68	3.34	3.45	2.36	1.44	1.34	1.04	1.16	1.36
11	-3.67	-22.5	20	8.15	7.85	3.54	2.09	1.16	1.09	0.93	0.93	1.10
12	-4.59	19.4	11	7.52	3.24	2.88	1.74	1.26	1.13	0.96	0.89	1.03
13	-3.97	-41.6	11.1	6.75	3.89	3.47	1.98	1.31	1.25	0.99	1.22	1.05
14	-5.43	-38.4	15.2	4.36	3.18	2.82	1.80	1.27	1.24	1.01	1.02	1.05
15	-3.4	-6.89	-24.8	-43.7	10.9	5.14	2.62	2.43	1.24	1.14	1.18	0.96
16	-5.2	-8.8	-28.9	12.5	6.66	3.62	3.05	2.01	1.59	1.34	1.19	0.94
17	-7.05	-48.1	21.3	14.6	6.05	2.85	2.21	1.663	1.391	1.04	1.12	1.17
18	-5.78	-13.1	101.6	16.2	5.11	4.03	2.51	1.54	1.300	1	1.19	0.99
19	-5.25	-10	-32.1	15.7	3.96	3.72	2.45	1.54	1.22	0.94	1.17	1.00

Lift/drag coefficient vs velocity & AOA

APPENDIX IV

Formulas used to calculate Lift Coefficient, Drag Coefficient and Reynolds Number

1. Coefficient of lift:

$$C_L = \frac{F_L}{\frac{1}{2} \rho V^2 A}$$

- Density of air, $\rho = 1.18 \text{ kg/m}^3$
- Free stream velocity, V
- Reference area, $A = 0.01018 \text{ m}^2$
- Force of lift, F_L

2. Coefficient of drag

$$C_D = \frac{F_D}{\frac{1}{2} \rho V^2 A}$$

- Density of air, $\rho = 1.18 \text{ kg/m}^3$
- Free stream velocity, V
- Reference area, $A = 0.01018 \text{ m}^2$
- Force of drag, F_D

3. Reynolds number

$$Re = \frac{\rho V L}{\mu}$$

- Density of air, $\rho = 1.18 \text{ kg/m}^3$
- Free stream velocity, V
- Chord length, $L = 0.09 \text{ m}$
- Viscosity of air, $\mu = 1.8395 \times 10^{-5} \text{ kg/m.s}$ at atmospheric temperature, $T=25^\circ$

